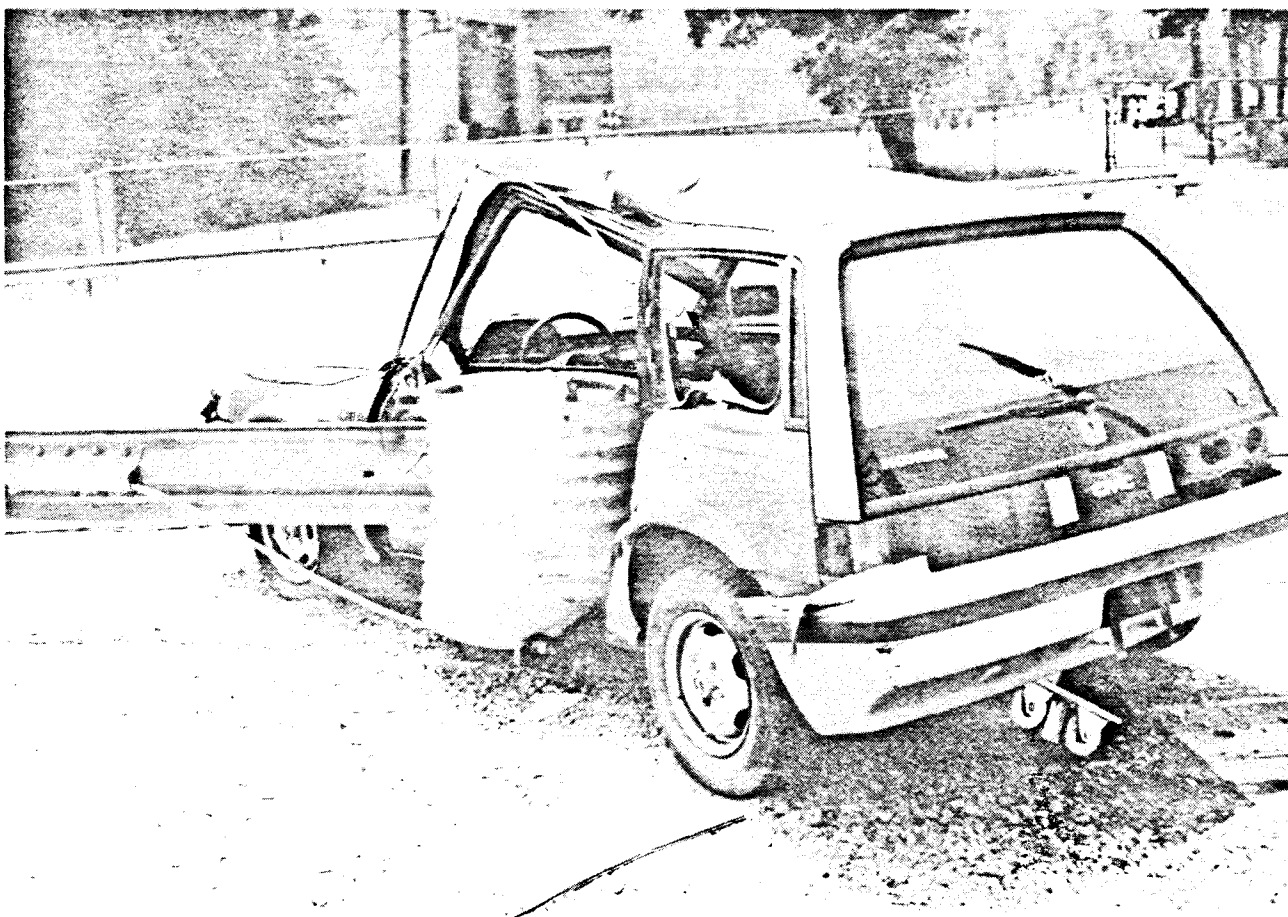




Side Impact Crash Testing of Roadside Structures

FHWA-RD-92-079

May 1993



U.S. Department of Transportation
Federal Highway Administration

Research and Development
Turner-Fairbank Highway Research Center
6300 Georgetown Pike
McLean, Virginia 22101-2296

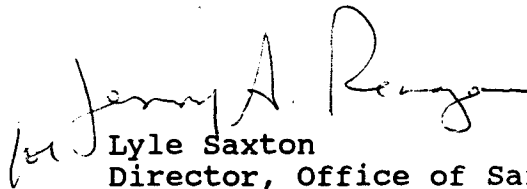
Reproduced by:
National Technical Information Service
U.S. Department of Commerce
Springfield, VA 22161

FOREWORD

This report documents a study to investigate the causes and severity of side impact collisions with fixed roadside objects like trees, utility poles and guardrails. This report is one of three that address various aspects of side impact collisions. The first report, Accident Data Analysis of Side-Impact Fixed Object Collisions (FHWA-RD-91-122), presents the results of an analysis of the Fatal Accident Reporting System (FARS) and National Accident Sampling System (NASS) accident data bases. The second report, Side Impact Test and Evaluation Procedures for Roadside Structure Crash Tests (FHWA-RD-92-062), presents recommendations for performing side impact crash tests of roadside appurtenances. The third report in this series, Side Impact Crash Testing of Roadside Structures (FHWA-RD-92-079), presents the results of a side-impact crash testing program involving luminaires supports and guardrail terminals.

This report (FHWA-RD-92-079) presents the results of a side-impact testing program performed at the Federal Outdoor Impact Laboratory. A total of 12 side impact crash tests were performed in this series. The tested appurtenances included the common slip-base luminaire support, the innovative Eqvist-Svenson-Vanke luminaire developed in Sweden as well as several variations of the breakaway cable terminal popular throughout the United States. The test results and those from other side-impact studies were used to build probabilistic models of the probability of serious injury as a function of basic crash test variables.

This report will be of interest to practicing engineers concerned with the design and testing of roadside hardware. The report will also be of interest to researchers and policy makers in assessing the performance of common roadside hardware in side impact collisions.



Lyle Saxton
Director, Office of Safety and Traffic
Operations Research and Development

NOTICE

This document is disseminated under the sponsorship of the Department of Transportation in the interest of information exchange. The United States Government assumes no liability for its contents or use thereof. This report does not constitute a standard, specification, or regulation.

The United States Government does not endorse products or manufacturers. Trade and manufacturers' names appear in this report only because they are considered essential to the object of the document.

1. Report No. FHWA-RD-92-079	2. Government Accession No.	3. Recipient's Catalog No.	
4. Title and Subtitle SIDE IMPACT CRASH TESTING OF ROADSIDE STRUCTURES		5. Report Date May 1993	
		6. Performing Organization Code	
7. Author(s) M.H. Ray and J.F. Carney III		8. Performing Organization Report No.	
9. Performing Organization Name and Address Vanderbilt University Department of Civil and Environmental Engineering Nashville, Tennessee 37235		10. Work Unit No. (TRAIS) 3A5F4032	
		11. Contract or Grant No. DTFH-61-88-R-00092	
12. Sponsoring Agency Name and Address Design Concepts Research Division Federal Highway Administration 6300 Georgetown Pike McLean, Virginia 22101-2296		13. Type of Report and Period Covered Final Report	
		14. Sponsoring Agency Code	
15. Supplementary Notes Contracting Officer's Technical Representative: Martin Hargrave, HSR-20			
16. Abstract This report contains a summary of 12 side impact crash tests performed at the Federal Outdoor Impact Laboratory (FOIL) to evaluate the performance of several types of roadside structures. The tests are described and results presented. The results of these tests are then combined with earlier test series and statistical models that predict dummy responses from test results are developed. These preliminary models could be used to evaluate the risk to occupants based on the response of hypothetical anthropometric dummies.			
17. Key Words Change in velocity ESV pole FOIL Crash testing Luminaire support Side impact		18. Distribution Statement No restrictions. This document is available to the public through the National Technical Information Service, Springfield, Virginia 22161.	
19. Security Classif. (of this report) Unclassified	20. Security Classif. (of this page) Unclassified	21. No. of Pages 82	22. Price

SI* (MODERN METRIC) CONVERSION FACTORS

APPROXIMATE CONVERSIONS TO SI UNITS

Symbol	When You Know	Multiply By	To Find	Symbol
LENGTH				
in	inches	25.4	millimeters	mm
ft	feet	0.305	meters	m
yd	yards	0.914	meters	m
mi	miles	1.61	kilometers	km
AREA				
in ²	square inches	645.2	square millimeters	mm ²
ft ²	square feet	0.093	square meters	m ²
yd ²	square yards	0.836	square meters	m ²
ac	acres	0.405	hectares	ha
mi ²	square miles	2.59	square kilometers	km ²
VOLUME				
fl oz	fluid ounces	29.57	milliliters	ml
gal	gallons	3.785	liters	l
ft ³	cubic feet	0.028	cubic meters	m ³
yd ³	cubic yards	0.765	cubic meters	m ³
MASS				
oz	ounces	28.35	grams	g
lb	pounds	0.454	kilograms	kg
T	short tons (2000 lb)	0.907	megagrams	Mg
TEMPERATURE (exact)				
°F	Fahrenheit temperature	$5(F-32)/9$ or $(F-32)/1.8$	Celsius temperature	°C
ILLUMINATION				
fc	foot-candles	10.76	lux	l
fl	foot-Lamberts	3.426	candela/m ²	cd/m ²
FORCE and PRESSURE or STRESS				
lbf	poundforce	4.45	newtons	N
psi	poundforce per square inch	6.89	kilopascals	kPa

APPROXIMATE CONVERSIONS FROM SI UNITS

Symbol	When You Know	Multiply By	To Find	Symbol
LENGTH				
mm	millimeters	0.039	inches	in
m	meters	3.28	feet	ft
m	meters	1.09	yards	yd
km	kilometers	0.621	miles	mi
AREA				
mm ²	square millimeters	0.0016	square inches	in ²
m ²	square meters	10.764	square feet	ft ²
m ²	square meters	1.195	square yards	ac
ha	hectares	2.47	acres	mi ²
km ²	square kilometers	0.386	square miles	
VOLUME				
ml	milliliters	0.034	fluid ounces	fl oz
l	liters	0.264	gallons	gal
m ³	cubic meters	35.71	cubic feet	ft ³
m ³	cubic meters	1.307	cubic yards	yd ³
MASS				
g	grams	0.035	ounces	oz
kg	kilograms	2.202	pounds	lb
Mg	megagrams	1.103	short tons (2000 lb)	T
TEMPERATURE (exact)				
°C	Celsius temperature	$1.8C + 32$	Fahrenheit temperature	°F
ILLUMINATION				
lx	lux	0.0929	foot-candles	fc
cd/m ²	candela/m ²	0.2919	foot-Lamberts	fl
FORCE and PRESSURE or STRESS				
N	newtons	0.225	poundforce	lbf
kPa	kilopascals	0.145	poundforce per square inch	psi

* SI is the symbol for the International System of Units. Appropriate rounding should be made to comply with Section 4 of ASTM E380.

Contents

Chapter 1. Introduction	1
Measures of Severity	1
Chapter 2. Vehicles, Devices, and Test Procedures	6
Vehicles	6
Dodge Colt and Plymouth Champ	6
Honda Civic	9
Volkswagen Rabbit	9
Devices	9
Enquist-Svensson-Vanke Pole	10
Slipbase Pole	12
Transformer-base Pole	12
Guardrail Terminals	15
Chapter 3. Side Impact Crash Testing	20
Test 91S001	20
Test 91S002	23
Test 91S003	26
Test 91S004	26
Test 91S005	29
Test 91S006	29
Test 91S007	31
Test 91S036	34
Test 91S037	37
Test 91S038	39
Test 91S046	41
Chapter 4. Severity Modelling	43
Introduction	43
Modelling Process	44
Occupant Risk Model	49
Thoracic Trauma Model	50
Head Injury Criteria	56
Model Refinements	61
Chapter 5. Summary	64
A. Side Impact Crash Tests of Roadside Objects	65
B. SAS Programs	72
References	76

List of Figures

1	FOIL side impact layout.	7
2	Geometrical properties of the ESV pole.	11
3	Geometrical properties of the slipbase pole.	13
4	Geometrical properties of the transformer-base pole.	14
5	Breakaway cable terminal.	16
6	Eccentric loader breakaway cable terminal (ELT).	17
7	Modified eccentric loader breakaway cable terminal (MELT).	18
8	MELT enhanced for side impacts.	19
9	Occupant and vehicle kinematics of test 91S001.	24
10	Occupant and vehicle kinematics of test 91S002.	25
11	Occupant and vehicle kinematics of test 91S003.	27
12	Occupant and vehicle kinematics of test 91S004.	28
13	Occupant and vehicle kinematics of test 91S005.	30
14	Occupant and vehicle kinematics of test 91S006.	32
15	Occupant and vehicle kinematics of test 91S007.	33
16	Occupant and vehicle kinematics of test 91S036.	36
17	Occupant and vehicle kinematics of test 91S037.	38
18	Occupant and vehicle kinematics of test 91S038.	40
19	Occupant and vehicle kinematics of test 91S046.	42
20	TTI versus the maximum external static crush.	52
21	Observed versus predicted TTI.	55
22	Six-point damage sketch for calculating C_{area}	58
23	Observed versus predicted HIC.	60

List of Tables

1	Properties of test vehicles.	8
2	Test poles characteristics.	10
3	Summary of 1985 and 1987 crash tests.	21
4	Summary of 1991 crash tests.	22
5	Summary of the terminal test conditions and results.	35
6	Side impact crash test parameters.	45
7	Probability of $AIS > 3$ thoracic injury.	54
8	Probability of $AIS > 3$ head injury.	59
9	Data elements required in side impact crash tests.	62

Chapter 1. Introduction

In the United States, 225,000 people are involved in side impact collisions with fixed roadside objects every year. One in 3 is injured and 1 in 100 is killed.^[1] This level of injury represents a societal loss of more than \$3 billion.^[2] Collisions with the sides of vehicles account for one quarter of the cases in both the National Accident Sampling System (NASS) and Fatal Accident Reporting System (FARS) data bases.

The National Highway Traffic and Safety Administration (NHTSA) and automobile manufacturers have expended a great deal of effort in recent years formulating and studying the side impact problem. These studies have focused on vehicle-to-vehicle side impacts and the thoracic trauma which usually occurs in such collisions. In side impacts with narrow objects, however, the important injury mechanisms can be quite different. In many cases, the occupant's head is the first portion of the body to contact the vehicle interior. If the occupant and struck object are aligned, the occupant effectively strikes the pole directly causing extremely large impulses very early in the impact event. Even breakaway luminaire supports have a high probability of fatally injuring the occupant since the occupant strikes the pole long before the pole breaks away. An understanding of this important impact scenario is vital to making effective design changes to the roadside structures and vehicles. Installing interior padding, for example, without strengthening the door structure may have little beneficial effect for occupants of vehicles involved in side impacts with narrow objects.

Measures of Severity

Crash tests provide important information about the performance of roadside structures. Roadside structures must manage impact loadings by either yielding, breaking away, or collapsing. The objective of all roadside safety hardware is to minimize the risk to vehicle occupants in a collision. Judging the risk of human trauma in a collision is very difficult. Several methods for estimating collision severity have evolved over the last several decades.

NCHRP Report 230 covers the test procedures and evaluation criteria to be followed in evaluating the effectiveness of roadside safety hardware.^[3] Full-scale crash testing programs are specified, and the performance of a device is judged on the basis of three factors: (i) structural adequacy, (ii) occupant risk, and (iii) vehicle trajectory after collision. The structural adequacy of an appurtenance is evaluated by its ability to interact with a selected range of vehicle sizes and impact conditions in a predictable and acceptable manner. The unit should remain intact during the impact so that detached debris will not present a hazard to traffic. The occupant risk evaluation of a highway appurtenance is a surrogate measure of the response of a hypothetical vehicle occupant during the impact. The vehicle kinematics are used to estimate the impact velocity and ridedown accelerations of the occupant and limiting values are recommended. Another essential crash test requirement of *Report 230* is that the impacting vehicle remain upright during and after

collision and that the integrity of the passenger compartment be maintained. The vehicle trajectory after collision is of concern because of the potential risk to other traffic. An acceptable vehicle trajectory after impact is characterized by minimal intrusion into adjacent traffic lanes.

The *Report 230* procedures for acquiring occupant risk data involve the numerical integration of acceleration-time data. Of primary concern are the magnitudes of the hypothetical occupant impact velocity with the interior of the vehicle and the maximum 10 ms average deceleration of the occupant following this impact. The recommended threshold values for lateral occupant impact velocity and ridedown deceleration are 30 ft/s (9.2 m/s) and 15 g's, respectively.

The value of the occupant impact velocity depends on the "flail" distance available before impact occurs. *Report 230* assumes the occupant to be a rigid body whose acceleration, a_o , can be expressed as:

$$a_o = a_v + a_{o/v} \quad (1)$$

where a_v is the acceleration of the reference frame moving with the vehicle and $a_{o/v}$ is the acceleration of the occupant relative to the moving reference frame.

Assuming an unrestrained occupant has no acceleration until colliding with the vehicle interior, the above equation becomes:

$$|a_{o/v}| = |a_v| \quad (2)$$

Furthermore, the velocity of the occupant, v_o , is:

$$v_o = v_v + v_{o/v} \quad (3)$$

where v_v is the velocity of the reference frame moving with the vehicle and $v_{o/v}$ is the velocity of the occupant relative to the moving reference frame. Since v_o is a constant vector, C , prior to impact with the vehicle interior, equation (3) becomes:

$$C = C - \int_{t_1}^{t_2} a_v dt + v_{o/v} \quad (4)$$

which yields:

$$v_{o/v} = \int_{t_1}^{t_2} a_v dt. \quad (5)$$

Equations (2) and (5) form the basis for calculating the occupant/compartment impact velocities and the ride-down accelerations given in *Report 230*.

Traditionally, these occupant risk criteria have been the most important factors in developing roadside hardware and evaluating tests. However, under side impact conditions, the roadside structure intrudes into the occupant compartment this flail space model is not adequate. The following versions of the flail space concept were used in this research:

- The usual flail space model using a 1-ft (0.3-m) flail space and a nondeforming passenger compartment.
- The usual flail space model using the actual flail space [6.5 in (165 mm)] and a nondeforming passenger compartment.
- The relative velocity between the left side of the occupant's head and the intruding door. This is determined using the onboard film data. The onboard films of all the tests were analyzed. The coordinates of the door interior, the left side of the dummy's head, and a reference point are taken on each frame of the film by using a film motion analyzer. Knowing that the time between two consecutive frames is 1/500 s, the displacements of the head with respect to the intruding door are computed, and the velocity of the head with respect to the intruding door is found.
- The "normalized" relative velocity between the left side of the occupant's head and the intruding door. The dummy is seldom in position in a crash test so a technique for normalizing the data had to be developed in order to compare tests. The normalized occupant risk approach assumes that the forces on the occupant are the same as in the actual test but the occupant's initial position is taken in the usual "in-position" location [i.e., a flail space of 6.5 in (165 mm)] and the occupant's velocity at impact is set to zero. The equation of displacement for the hypothetical occupant is found by using the displacement data from the vehicle accelerometers and assuming the occupant is positioned 6.5 in (165 mm) from the interior of the door at the impact time. The equation of the door displacement is found from film analysis or using a displacement transducer. The normalized velocity is found by differentiating the difference between the two equations.
- The maximum closing velocity between the occupant's head and the intruding door. The maximum velocity can happen any time between the impact with the pole and vehicle and the impact between the occupant and the door.

Another important measure of occupant risk deals with injuries to organs within the thoracic cage. Damage to the liver, kidneys, and/or spleen can be life threatening.

Extensive lateral impact tests have been performed on human cadavers and surrogate specimens to determine physiological responses and develop an injury index. The result is Thoracic Trauma Index (TTI), which can be expressed in the form:^[4]

$$TTI(d) = 0.5(G_r + G_{ls}) \quad (6)$$

where G_r is the greater of the peak of either the upper or lower rib acceleration in g's and G_{ls} is the lower spine peak acceleration in g's. The TTI defined in equation 6 is that measured by the dummy. The TTI for a human includes an additional term which is a function of the age of the occupant. Federal Motor Vehicle Safety Standard No. 214 requires that the TTI not exceed 90 for two-door vehicles.^[5]

The TTI is not the only possible measure of thoracic trauma. Researchers at General Motors Research Laboratory, for example, developed a competing injury scale, the viscous criteria (VC).^{[6],[7]} Unfortunately, the data required to calculate VC are only obtainable using BioSID dummies which were not available in any of the side impact crash tests performed to date at the FOIL. In contrast, the TTI can be calculated using the more common Part 572 SID. Since most of the FHWA tests and all of the NHTSA tests contained data that could be used to calculate the TTI, the TTI was preferred as a measure of thoracic occupant trauma.

The TTI has been related to the probability of various levels of injury using the Abbreviated Injury Score (AIS).^[8] The cumulative density function of TTI was found to be a Weibull extreme value distribution.^[9] A $TTI = 90$ corresponds to a 0.16 probability of an $AIS > 3$ injury, assuming a population weighted average probability of injury.

Head injuries have been recognized for many years as one of the most debilitating types of trauma experienced in accidents. Injuries sustained by the head and brain are difficult to treat and often result in long-term disfunction. Such injuries often involve great cost to society either because of losses due to an early death or the costs of long-term treatment and loss of productivity. In the United States it is estimated that approximately 135,000 persons are hospitalized each year for brain injuries as a result of motor vehicle accidents. The in-hospital costs of these injuries is on the order of \$370 million. In a recent examination of 49,143 trauma patients in 95 trauma centers, Gennarelli *et al.* discovered that although patients with head injuries accounted for one third of the trauma cases they represented two thirds of the trauma deaths.^[10]

Tests on embalmed cadaver heads have led to the following Head Injury Criteria (HIC):^[11]

$$HIC = \left[\frac{1}{t_2 - t_1} \int_{t_1}^{t_2} a dt \right]^{2.5} (t_2 - t_1) \quad (7)$$

where a is the resultant head acceleration, and t_1 and t_2 are two points in time during any interval in which the head is in continuous contact with a part of the vehicle other than the belt system. Values of HIC greater than 1000 are to be avoided.

$HIC = 1000$ implies a risk of $AIS > 3$ injury of 0.18: 18 percent of occupants with a $HIC = 1000$ will be severely injured.^[12] The limits commonly accepted for HIC and TTI represent similar levels of risk for both injury mechanisms.

Unfortunately, the HIC was not developed to measure head injury potential in side impacts. The differences between longitudinal and lateral head impact tolerance and the degree to which the Part 572 head form predicts human injury have been debated but no consensus has been reached.^[13] It is widely agreed, however, that the head is probably *less* tolerant in lateral impacts than in frontal impacts so the HIC should certainly be no greater than 1000. There is a great need for the biomechanics research community to address the issue of an appropriate lateral HIC limit or, more generally, head injury criteria for the side of the head.

The purpose of this report is to provide a summary of side impact crash tests and develop preliminary side impact severity modeling for roadside hardware. This first chapter serves as an introduction and reviews the occupant risk criteria recommended in *Report 230* and other measures of injuries related to the thoracic and head areas of the body. Descriptions of the vehicles, devices, and test procedures employed in side impact crash testing are presented in chapter 2. Chapter 3 summarizes the results and characteristics of individual side impact crash tests. This technical data is employed in chapter 4 to develop appropriate severity models to evaluate side impact crash testing.

Chapter 2. Vehicles, Devices, and Test Procedures

The side impact tests described in this report were conducted at the Federal Outdoor Impact Laboratory (FOIL). The side impact test layout is illustrated in figure 1. A dual rail guidance and delivery system is employed during side impact testing with the majority of the vehicle weight supported by the main rail and the remainder supported by the an auxiliary outrigger rail. The vehicle rolls on casters bolted to the undercarriage of the vehicle. Just prior to impact, the dual rail system terminates so as the vehicle approaches the test article, it falls off the end of the rail system, lands on the ground, and skids sideways on its tires until impact.

Vehicles

With several exceptions, only standard Report 230 1800S vehicles have been used in side impact crash testing to evaluate the principal performance factors of structural adequacy, occupant risk, and vehicle trajectory after each side impact collision. Small cars at low speeds are critical tests when impacting breakaway or combinations yielding supports because the available kinetic energy is minimized. The door configuration is an important design characteristic. The two-door design offers a longer door and a softer force-deformation curve, while the four-door car is usually stiffer. Two-door Dodge Colts, Plymouth Champs, Honda Civics, and VW Rabbits have been used in this research. Inertial properties of the test vehicles are shown in table 1.

Dodge Colt and Plymouth Champ

Dodge Colts and Plymouth Champs have test inertial weights of 1,850 lb (8.2 kN), and the gross static weight when the anthropometric dummy is included in the vehicle is 2,015 lb (9.0 kN). The longitudinal center of gravity of the vehicle without the occupant is located 32 in (813 mm) behind the centerline of the front axle. Inertial measurements of Dodge Colt vehicles were performed at the FOIL in earlier contracts and are shown in table 1.^{[14],[15]}

This test series of side impacts with slipbase poles used 1980 through 1982 Colts. This model changed body styles slightly in 1985 so the latest test series used primarily 1981 through 1985 Dodge Colts in order to match the vehicles in the earlier test series.

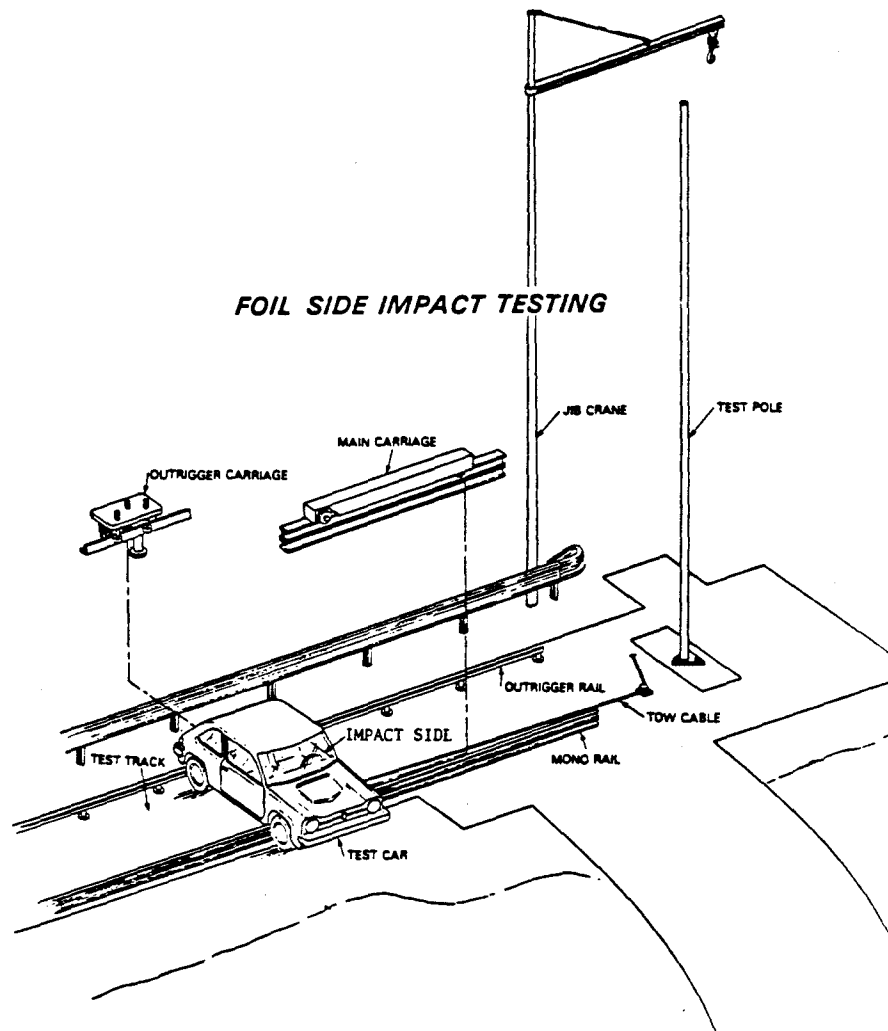


Figure 1. FOIL side impact layout.

Table 1. Properties of test vehicles.

Actual Test Vehicle			
Vehicle	Dodge Colt	Honda Civic	VW Rabbit
Delivered Weight (lb)	1,920	1,920	1,845
As tested weight, inertial (lb)	1,850	1,850	1,850
As tested weight, gross (lb)	2,015	2,015	2,015
Average As-Delivered Properties			
Delivered cg-x: behind front axle centerline (in)	32	35	32.5
Delivered cg-y: behind vehicle centerline (in)	0.0	0.0	0.0
Delivered cg-z: above ground (in)	20.0	20.5	21
Delivered Roll Inertia (slug-ft ²)	205	174	199
Delivered Pitch Inertia (slug-ft ²)	822	903	814
Delivered Yaw Inertia (slug-ft ²)	880	1,033	893
Average As-Tested Properties			
As tested cg-x: behind front axle center line (in)	32	—	32.5
As tested cg-y: behind vehicle center (in)	0.0	—	0.0
As tested cg-z: above ground (in)	20.2	—	20
As tested Roll Inertia (slug-ft ²)	196	—	204
As tested Pitch Inertia (slug-ft ²)	769	—	769
As tested Yaw Inertia (slug-ft ²)	844	—	889

$$1 \text{ lb} = 4.448 \text{ N} = 0.45 \text{ kg}$$

$$1 \text{ in} = 25.4 \text{ mm}$$

$$1 \text{ slug} = 14.59 \text{ kg}$$

$$1 \text{ ft} = 0.305 \text{ m}$$

Honda Civic

As was the case with the Colts, the test inertial weights of the Honda Civics was 1,850 lb (8.2 kN), and the gross static weight when the anthropometric dummy was included in the vehicle was 2,015 lb (9.0 kN). The longitudinal center of gravity of the vehicle without the occupant is located 35 in (889 mm) behind the centerline of the front axle.

The Honda Civic was chosen for certain tests to investigate the effect of employing a door structure stronger than the Dodge Colt on the dynamic response of the device, vehicle, and test dummy. NHTSA tests of the compliance of production vehicles to the 1970s version of FMVSS 214, indicated the Honda Civic had a stronger door design than the Dodge Colt.

Volkswagen Rabbit

The Volkswagen Rabbit was also used in impacts with rigid poles in earlier contracts.^[15] The test inertial weight for the vehicle is 1,845 lb (8.2 kN). The longitudinal center of gravity of the vehicle without any occupant is located 32.5 in (826 mm) behind the centerline of the front axle.

Devices

Breakaway and yielding luminaire and sign supports are devices that are designed to readily disengage, fracture, or bend away from an impacting vehicle upon impact. The safety performance objective of these devices is to smoothly stop the vehicle, or permit the vehicle to pass without subjecting occupants to injury producing forces. Three types of luminaire supports have been evaluated in full-scale side-impact crash tests: a slipbase pole, a transformer base pole, and the Enquist-Svensson-Vanke pole (ESV).^[16] The ESV pole was chosen because of its unique collapse mechanism. This type of pole stops a vehicle by dissipating energy. The cross section of the pole is flattened by the striking vehicle and energy is dissipated by plastically deforming the pole. The slipbase and transformer base poles were chosen because they represent the most common types of breakaway luminaires used on U.S. highways. Luminaire supports developed during the past several decades in the United States have tended to use either slip-base or frangible-base technologies. Frangible-base and slip-base poles operate by detaching the pole from a base. The detached luminaire support is then free to rotate away from the vehicle. Ideally, the vehicle passes by with little change in velocity after activating the slip or breakaway mechanism. Physical properties and dimensions of the devices are contained in table 2.

Table 2. Test poles characteristics.

Device	ESV	Slipbase pole	Transformer pole
Manufacturer:	Varmforzinkning; Smalandsstenar Sweden	Ameron	Union Metal
Base Type:	ESV	California type 31 slipbase	Transformer
Material:	Galvanized steel	steel	steel
Total Weight: (lb)	219	416	386
Luminaire Weight: (lb)	150	51	51
Height, c.g.:	19 ft	21 ft	23 ft 10 in
Top diameter: (in)	4	3-1/2	6
Bottom diameter: (in)	8	7-1/2	8
Mast Arm Length:	6 ft	15 ft 10 in	14 ft 9 in
Luminaire Height:	32 ft 10 in	35 ft 10 in	39 ft
Number of bolts:	4	3	4
Size: Diameter	1-in	1-in	1-in

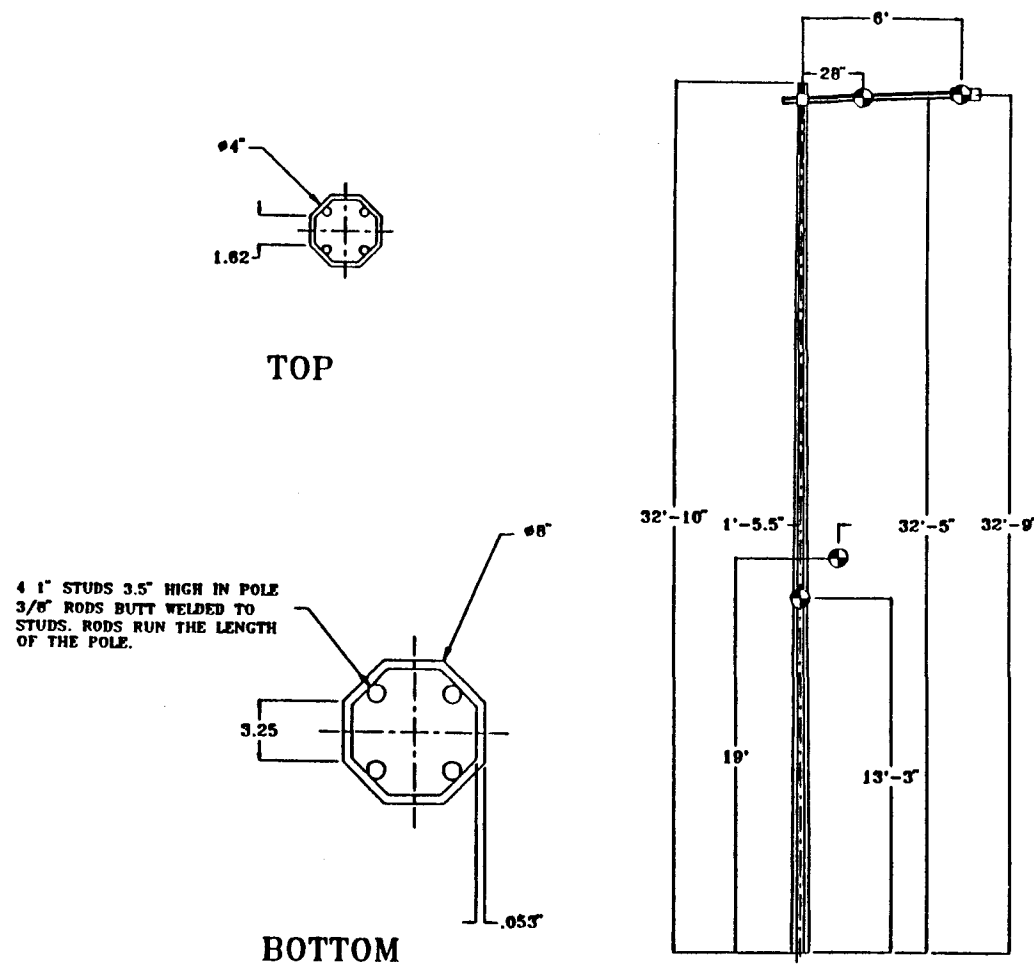
1 lb = 4.448 N

1 ft = 0.305 m

1 in = 25.4 mm

Enquist-Svensson-Vanke Pole

The ESV pole stops a vehicle by absorbing energy. The cross section of the pole is flattened by the striking vehicle and energy is dissipated by deforming the pole. The ESV pole was developed in Sweden during the late 1970's. The collapse mechanism has been designed so that the occupant response in a frontal collision is well below the threshold of serious injury. In over a decade of use throughout Scandinavia there have been no fatalities reported in accidents involving ESV-like poles.^[16] By changing the dimensions of pole the energy dissipation can be optimized for different vehicle masses and speeds. Figure 2 shows the design features of the ESV pole used in the tests discussed in chapter 4. The outside of the pole is a hexagon formed from 0.053-in (1.35-mm) thick steel sheet. Four 3/8-in (9.5-mm) diameter round steel rods are tack welded to the inside of the steel skin. The four rods are butt-welded to 1-in (25-mm) diameter anchor rods. The pole can be installed using either a soil mounted anchor or by directly attaching it to a rigid base. The test poles were fixed to the universal rigid support at the FOIL. This support is a 2-in (51-mm) thick steel plate. The poles that were delivered for testing in this project were for soil mounted applications so the anchor rods were shortened to allow them to be attached to the universal support. Rigid, deck-mounted supports similar to the ones used in these tests are also common in Scandinavia.



WEIGHTS (LB)

POLE: 150

MAST ARM: 15

MAST ARM 2: 4

LUMINAIRE: 50

TOTAL ASSY: 219

POLE PARAMETERS

BASE DIA.: 8 in

TIP DIA.: 4 in

POLE B.C. DIA.: 6 3/4 in

WALL THICK (IN): .053

MATERIAL: GALV. STEEL

1 in = 25.4 mm
1 ft = 0.305 m
1 lb = 4.448 N

Figure 2. Geometrical properties of the ESV pole.

In a collision, the tack welds fracture and the cross section flattens. The flattened section is then pulled around the bumper or sill, continuously flattening the cross section. Energy is absorbed by the flattening and wrapping of the pole around the vehicle. Physical properties and dimensions of the ESV pole are contained in table 2. Four side impact crash tests were performed on the ESV pole in this research.

Slipbase Pole

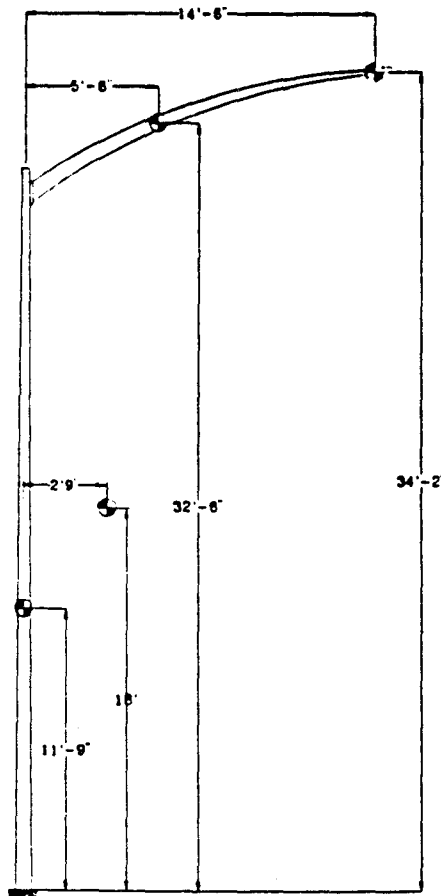
The slipbase pole was chosen since it was known to induce a momentum change during frontal impacts which has traditionally been considered acceptable. Luminaire supports developed during the past several decades in the United States have tended to use either slipbase or frangible-base technologies. Frangible-base and slipbase poles operate by detaching the pole from the base. When performing properly, the vehicle passes by with little change in velocity.

The slipbase pole is one of the better performing devices on the highway system. The geometrical properties of the pole are shown in figure 3. The California type 31 slipbase support was used in this research. It uses a triangular 3-bolt slipbase. The slip base was positioned so impact would occur parallel to an edge which had two bolts aligned. The luminaire support had a mast arm attached during these tests as well as a steel and plywood weight attached to the end of the arm to simulate the light fixture. The slipbase was clamped together with three strain gauged bolts which were tightened prior to the test. Physical properties and dimensions of the breakaway luminaire support are contained in table 2. Three side impact crash tests with slipbase poles were performed in this research. Fifteen more side impact tests were performed in earlier contracts using the slipbase pole.^{[15],[17],[14]}

Transformer-base Pole

The transformer base pole is made from aluminum which is suppose to fracture upon impact. The physical properties of the this type of luminaire support are also contained in table 2. The luminaire support had a mast arm attached during this test as well as a steel weight attached to the end of the arm to simulate the mass of a light fixture. The base was clamped to the base plate with studs and nuts which were tightened to 200 ft-lb (271 N-m) of torque just prior to the test. The mechanical properties of the pole are shown in figure 4. One side impact crash test was performed in an earlier contract.^[15]

Seven side impact tests involving rigid instrumented poles have been performed by various agencies (see appendix A). These tests were very useful for determining the load paths within the vehicle. The contribution of the sills, door, and roof rail could be assessed using information obtained from load cells on the instrumented pole.



MANUFACTURER: AMERON

WEIGHTS (LB)

POLE: 280

MAST ARM: 75

LUMINAIRE: 50

TOTAL ASSY.: 415

POLE PARAMETERS

BASE DIAMETER: 8 in

TIP DIAMETER 3 7/8 in

WALL THICKNESS 3/16 in

MATERIAL: GALV. STEEL

SLIP BASE PARAMETERS

BASE TYPE: CA-31

NUMBER OF SLIP BOLTS: 3

SLIP B.C. DIAMETER: 15 in

DIAMETER OF SLIP BOLTS: 1 in

NUMBER OF FOUNDATION BOLTS: 3

FOUNDATION B.C. DIAMETER: 15 in

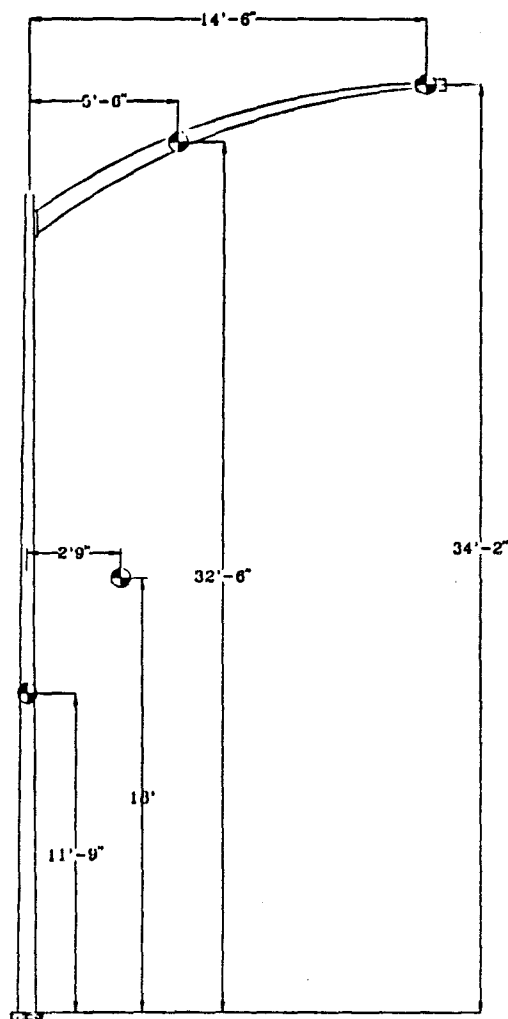
SLIP BOLT CLAMP FORCE: 14 kips (6 kips 91S006)

KEEPER PLATE: YES

SLIP BASE THICKNESS 1.5 in

1 in = 25.4 mm
1 ft = 0.305 m
1 lb = 4.448 N

Figure 3. Geometrical properties of the slipbase pole.



MANUFACTURER: AMERON

WEIGHTS (Lb)

POLE: 290

MAST ARM: 75

LUMINAIRE: 50

TOTAL ASSY.: 415

POLE PARAMETERS

BASE DIAMETER: 8 in

TIP DIAMETER: 3 7/8 in

WALL THICKNESS 3/16 in

MATERIAL: GALV. STEEL

SLIP BASE PARAMETERS

BASE TYPE: CA-31

NUMBER OF SLIP BOLTS: 3

SLIP B.C. DIAMETER: 15 in

DIAMETER OF SLIP BOLTS: 1 in

NUMBER OF FOUNDATION BOLTS: 3

FOUNDATION B.C. DIAMETER: 15 in

SLIP BOLT CLAMP FORCE: 14 kips (6 kips 91S006)

KEEPER PLATE: YES

SLIP BASE THICKNESS: 1.5 in

1 in = 25.4 mm
1 ft = 0.305 m
1 lb = 4.448 N

Figure 4. Geometrical properties of the transformer-base pole.

Guardrail Terminals

In addition to the tests with the poles described above, tests were performed on the following four guardrail terminals:

- Breakaway cable terminal (BCT).
- Eccentric loader breakaway cable terminal (ELT).
- Modified eccentric loader breakaway cable terminal (MELT).
- Modified eccentric loader terminal enhanced for side impact (MELT-SI).

The BCT is a standard breakaway cable terminal as described in FHWA Technical Advisory T 5040.25.^{[18],[19]} Figure 5 shows a photograph of this system. The BCT is one of the most common terminals used with W-beam guardrails. This device was selected to explore the side impact performance of typical guardrail terminals in use today. The BCT was developed in the early 1970's to provide a safe method for terminating guardrails.^[20] In an end-on collision, the BCT posts fracture allowing the W-beam to buckle. The vehicle is impulsively directed either in front of or behind the barrier. This process is often called "gating." The terminal is also designed so that it provides the required anchorage for impacts downstream from the end. The BCT must be strong enough to serve as an anchor in mid-length collisions while breaking away in end-on collisions.

The ELT is a derivative of the BCT that was developed to provide improved performance in collisions with smaller passenger cars.^{[20],[21],[22]} Figure 6 shows the details of this device.

The nose piece of the BCT was replaced with a culvert section containing a loader arm. When hit head-on this loader arm introduces a buckling load into the W-beam. The W-beam is not bolted to the rail in the first 25 ft (7.6 m) of guardrail so the beam is essentially unsupported once the first post breaks. The large unsupported length makes the buckling load for the W-beam very low. This low buckling load minimizes the resistance to the striking vehicle. The post placement is slightly different than the placement used in the BCT. A sharper parabolic curve is used to further enhance the buckling action of the W-beam. The usual BCT anchor cable is included to provide a tensile reaction in downstream collisions. A spreader bar is located between the first and second posts to distribute the downstream foundation load over the first two posts.

The MELT is shown in figure 7. The MELT is the latest variation of the breakaway cable terminal family of W-beam guardrail end treatments.^[20] The MELT borrows some of the features of the ELT like a sharper parabolic flare and a laterally unsupported W-beam section near the end of the terminal. The nose element is similar to the BCT nose except horizontal baffle plates are added to stiffen the nose element and provide a moment arm

that will buckle the laterally unsupported W-beam. In an end-on collision, the first two posts fracture allowing the W-beam to buckle. The vehicle is impulsively directed either in front of or behind the barrier. This process is called "gating." The terminal is also designed so that it provides the required anchorage for impacts downstream from the end. The MELT must be strong enough to serve as an anchor in mid-length collisions while breaking away in end-on collisions.

An enhanced version of the MELT specifically designed to activate in a side impact collision (MELT-SI) was also tested (see figure 8).^[23] Several additional changes were made to the enhanced MELT design to improve its side impact performance.

All the design changes were intended to promote early loading of the first post and beam. Acceptable performance would not be possible unless the first post broke early in the event and the beam buckled. The design details of the enhanced MELT are presented in Test Report FHWA-RD-92-052.

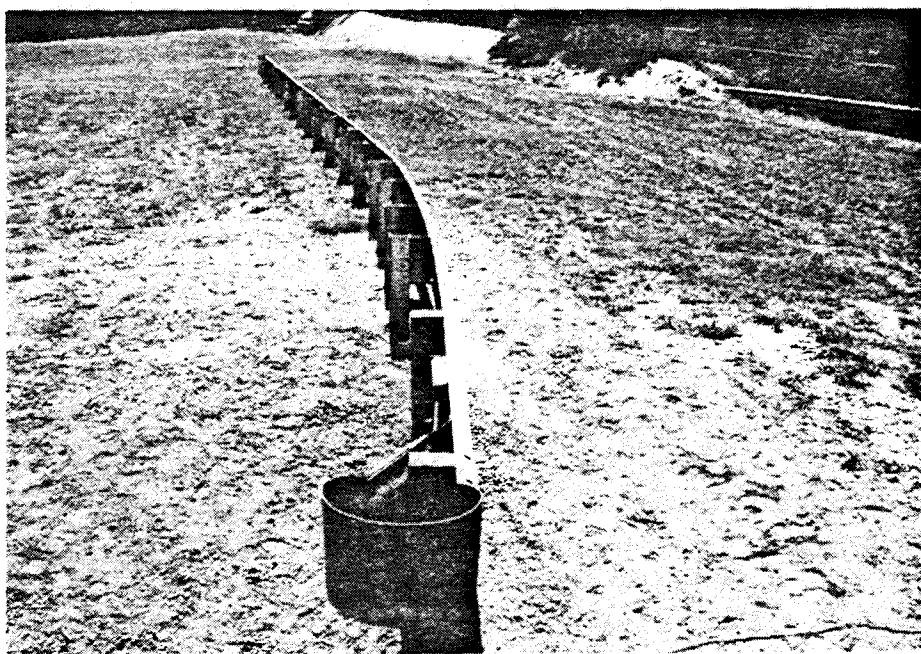


Figure 5. Breakaway cable terminal.

Reproduced from
best available copy.



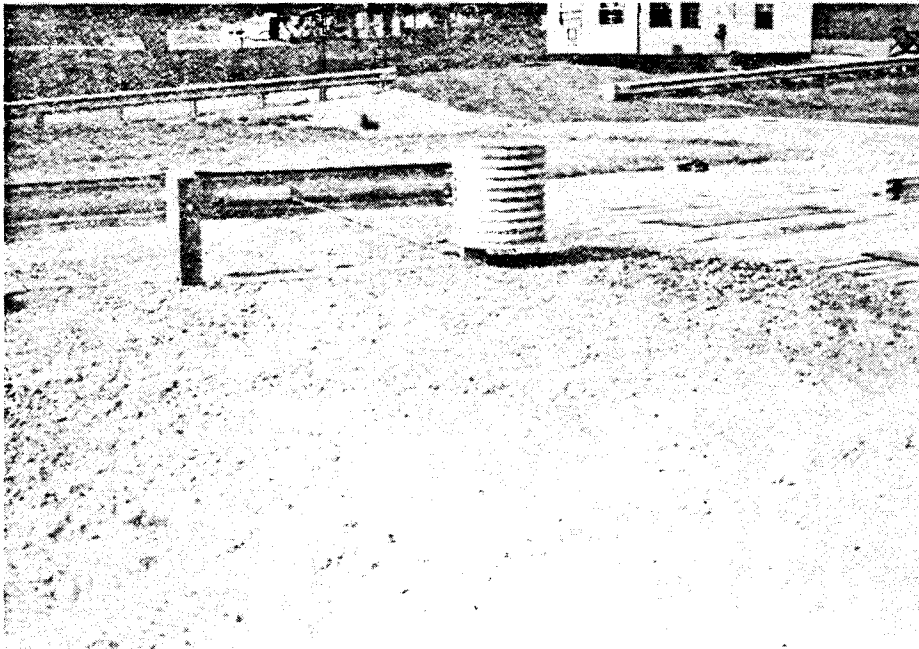
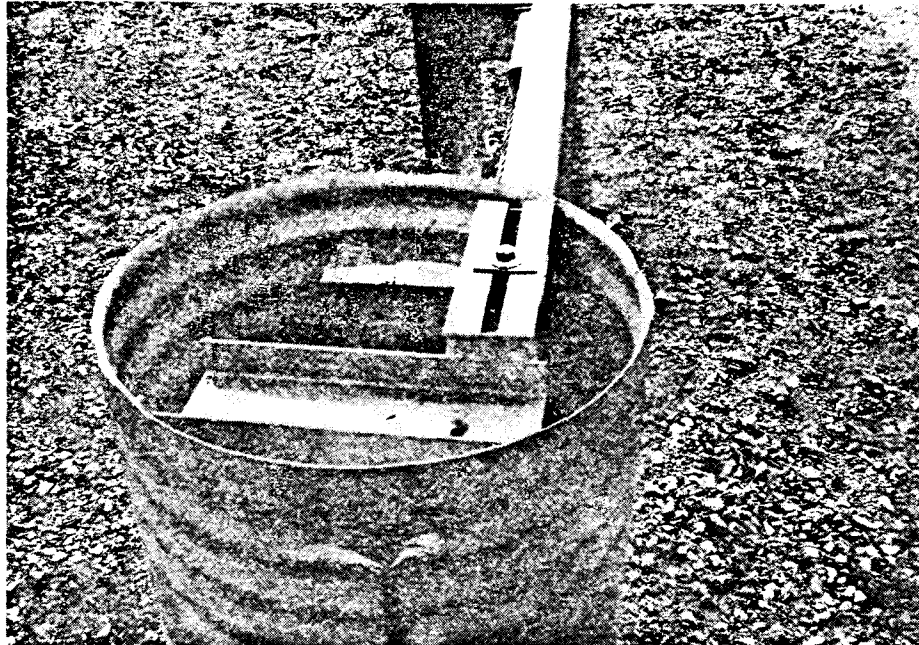


Figure 6. Eccentric loader breakaway cable terminal (ELT).

Reproduced from
best available copy.





Figure 7. Modified eccentric loader breakaway cable terminal (MELT).

Reproduced from
best available copy.



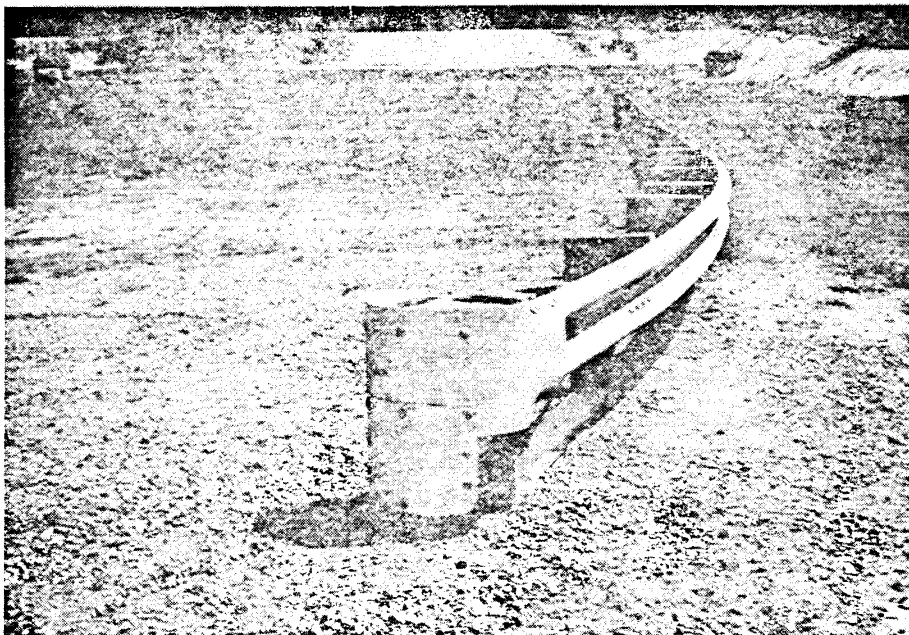
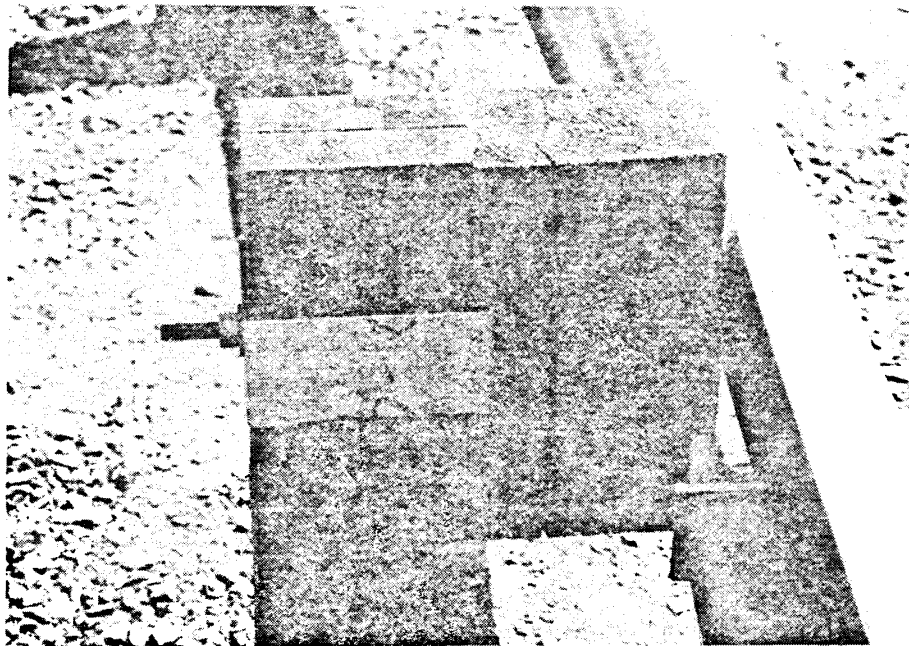


Figure 8. MELT enhanced for side impacts.

Reproduced from
best available copy.



Chapter 3. Side Impact Crash Testing

Side impact crash testing involving narrow hazards is a relatively new phenomenon. The earliest known test was performed in the United Kingdom in 1967. No such tests were conducted in the United States prior to 1977. Since that time, approximately 30 tests have been run at the FHWA's FOIL facility. Small 1800S automobiles were employed in most of these tests. Impacted devices have included rigid poles, slipbase luminaire supports, a transformer base pole, ESV poles, a BCT, an ELT, a MELT, and a MELT-SI.

Forty-four side impact crash tests of roadside objects have been performed throughout the world since 1967. Appendix A contains a list of all known side impact crash tests of roadside hardware. Thirty of these tests were performed at the FOIL since 1982. The data from 15 of these 30 FOIL tests are used in the next chapter to develop side impact severity models. Fifteen tests were eliminated from the data base for a variety of reasons including data acquisition failures, missing data and/or dummies, and nonstandard vehicles. Sixteen pole tests are summarized below and are divided into two parts. Table 3 presents the results of side impact tests conducted in 1985 and 1987 at the FOIL. Table 4 summarizes seven side impact FOIL pole tests which took place in 1991. In addition to these seven side impact tests with poles, the test program included the four terminal tests described above and one frontal test into a rigid pole. The 11 side impact tests are summarized in the next section.

Test 91S001

The test vehicle was a 1983 Dodge Colt and the pole was a 32.8-ft (10-m) ESV luminaire support. The impact occurred at 29.9 mi/h (48.1 km/h) at a point on the left door in line with the shoulder of the occupant. Upon impact the vehicle's driver side door began to crush and the pole started to collapse. As the impact event progressed the vehicle began to yaw counter-clockwise, continuing forward and away from the impact point after yawing a total of 93 degrees. Its final resting position was approximately 5 ft (1.5 m) to the right and 12 ft (3.7 m) downstream of the impact point.

The vehicle was extensively damaged during the collision. The maximum residual crush of the vehicle at the impact point was 16 in (406 mm). The intrusion event occurred over 60 ms. The pole was also extensively damaged. On impact, the pole activated and began to wrap around the sill and door structure. Approximately 4 ft (1.2 m) of the pole was flattened and had been pulled over the sill. As the impact event progressed, the inertia of the pole caused a buckle to form about 15 ft (4.6 m) up the pole. One of the butt-welded connections between the 3/8-in (9.5-mm) rods and the 1-in (25.4-mm) anchor bolts fractured. The galvanized sheet around the base was torn in several places.

Table 3. Summary of 1985 and 1987 crash tests.

Test Number	1469-SI-4-85	1469-SI-6-85	1785-SI-2-87	1785-SI-3-87	1785-SI-4-87	1785-SI-5-87	1785-SI-6-88	1785-SI-7-88	1785-SI-8-88
Vehicle type	Honda Civic	Dodge Colt	Dodge Colt	Dodge Colt	Plymouth Champ	Plymouth Champ	Plymouth Champ	Dodge Colt	Plymouth Champ
Structure	luminaire support	luminaire support	transformer base	slipbase pole	slipbase pole	slipbase pole	slipbase pole	slipbase pole	slipbase pole
Gross vehicle weight (lb)	1,964	1,962	2,010	2,007	2,010	2,010	2,010	2,007	2,008
Actual impact velocity (mi/h)	29.4	30.1	28.64	30.5	30.48	29.7	28.25	28.9	29.6
Impact location	on shoulder	on shoulder	on shoulder	on shoulder	on shoulder	12 in behind shoulder	12 in ahead of shoulder	24 in ahead of shoulder	on shoulder
Maximum vehicle crush (in)	10.5	17.25	26	9.5	10	13	36	7.7	7.5
Yaw angle (degrees)	90	90	90	90	90	90	90	90	90
Ridedown acceleration (g)	3.7	1.4	8.35	2.28	1.47	3.09	4.9	3.5	1.99
12-in flail occupant impact velocity (ft/s)	15.6	9.8	26.67	6.13	9.11	11.4	28.8	14.7	7.11
Actual occupant impact velocity (ft/s)	24.5	19	33	10.3	13	17	14.5	12.5	17.6
Intrusion time (s)	0.072	0.09	0.138	0.078	0.078	0.078	0.156	0.15	0.078
Intrusion rate (in/s)	145	191	185	122	128	167	230	51.3	96.15
Occupant lateral position (in)	3.8	4.2	4.7	2.12	2.45	1.9	5.2	3.3	3.93
HIC	2827	9307	3385	8684	8026	64	2191	150	1996
TTI (g's)	217	233	291	224	192	58	126	14	91

1 lb = 4.448 N = 0.45 kg
 1 in = 25.4 mm
 1 mi/h = 1.61 km/h
 1 ft/s = 0.305 m/s

Table 4. Summary of 1991 crash tests.

Test Number	91S001	91S002	91S003	91S004	91S005	91S006	91S007
Vehicle type	Dodge Colt	Dodge Colt	Honda Civic	Plymouth Champ	Dodge Colt	Dodge Colt	Dodge Colt
Structure	ESV pole	ESV pole	ESV pole	Slipbase pole	ESV pole	Slipbase pole	Slipbase pole
Gross vehicle weight (lb)	2015	2015	2015	2015	2015	2015	2015
Actual impact velocity (mi/h)	29.9	17.8	29.9	18.9	41.5	20.8	39.8
Impact location	on shoulder	on shoulder	on shoulder	on shoulder	on shoulder	on shoulder	on shoulder
Maximum vehicle Crush (in)	16.0	9.0	8.5	18.75	10	10	13
Yaw angle (degrees)	90	90	90	90	90	90	90
Ridedown acceleration (g)							
for 12 in flail (g's)	4.36	2.3	2.38	11.6	6.72	2.9	5.48
for 6.5 in flail (g's)	4.36	4.1	4.23	16.5	6.72	7.13	5.48
Occupant impact velocities							
for 12 in flail (ft/s)	13.4	14	8.4	23.75	17.6	13.3	11.11
for 6.5 in flail (ft/s)	13	11.7	8.2	18.55	13.8	10.9	8.36
Actual occupant impact velocity (ft/s)	15	25.6	12	26.4	14	28.8	19
Normalized velocity (ft/s)	20	14	7	20.0	10	17	22
Intrusion time (s)	0.06	0.06	0.06	0.09	0.035	0.06	0.04
Intrusion rate (in/s)	267	150	142	209	285	167	325
Actual ccupant lateral position (in)	11.5	0.0	3.0	0.0	7	0.0	2.2
HIC	398	44101	503	2513	139	NA	17776
TTI (g's)	145	47	97	82	109	NA	413

1 lb = 4.448 N = 0.45 kg
 1 in = 25.4 mm
 1 mi/h = 1.61 km/h
 1 ft/s = 0.305 m/s

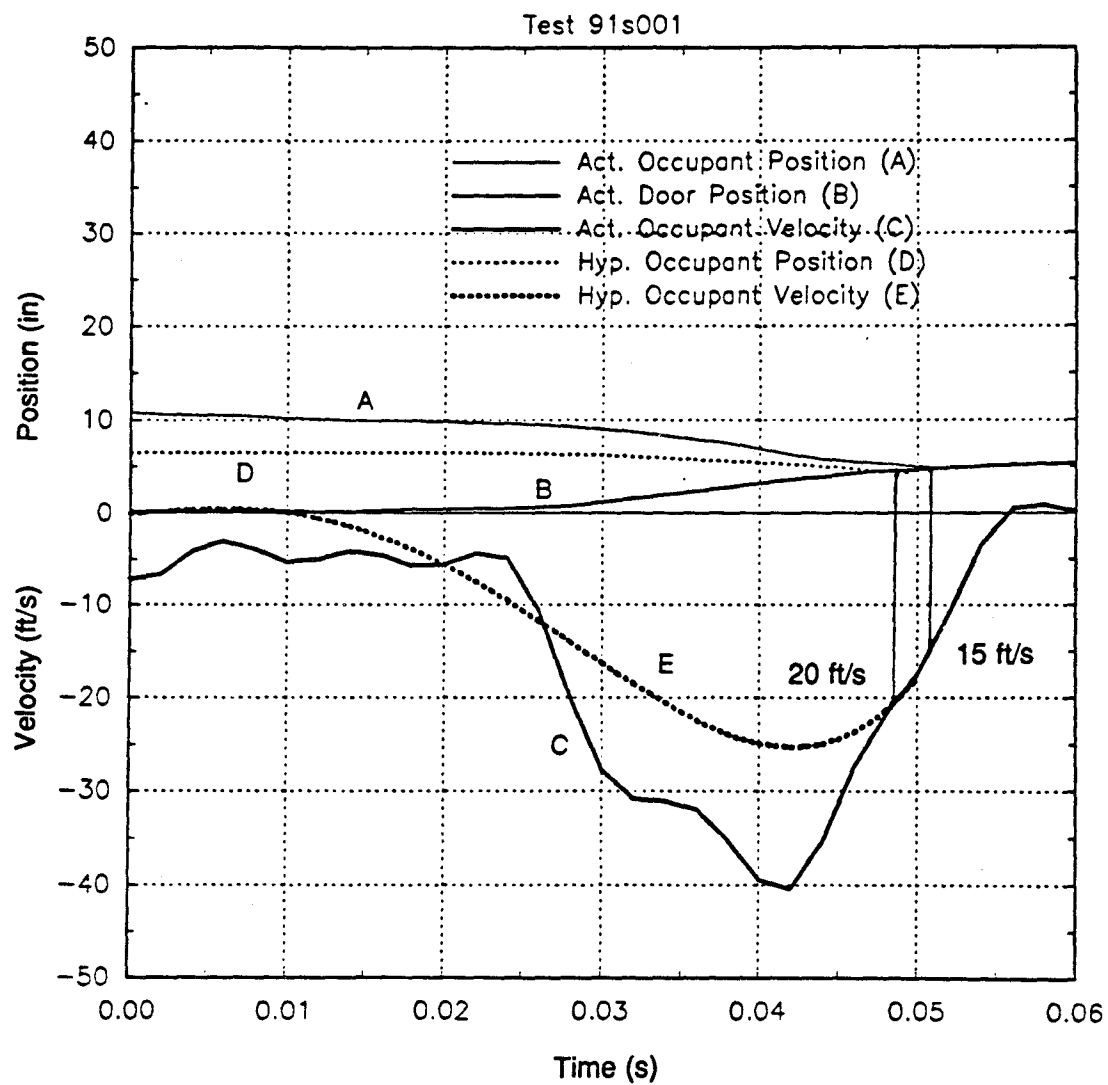
Just prior to impact, the dummy was slightly out of position, leaning in-board. The actual fail distance at impact was 11.5 in (292 mm) rather than 6.5 in (165 mm). After impact the dummy rapidly accelerated toward the door, striking the window and the intruding pole. The actual impact velocity of the occupant with the interior of the vehicle was 15 ft/s (4.6 m/s). Figure 9 shows a graph of the positions of the occupant and the door interior during the impact event. The TTI was found to be 145, which is greater than the limit of 90 specified by NHTSA in the amended FMVSS 214. The HIC observed in the test was 398, well below the usual limit of 1,000.

This collision should probably be rated as unacceptable because of the high TTI value. It should be noted, however, that the HIC was quite low, and the vehicle response was stable. Furthermore all calculated occupant impact velocity values were below the limit of Report 230.

Test 91S002

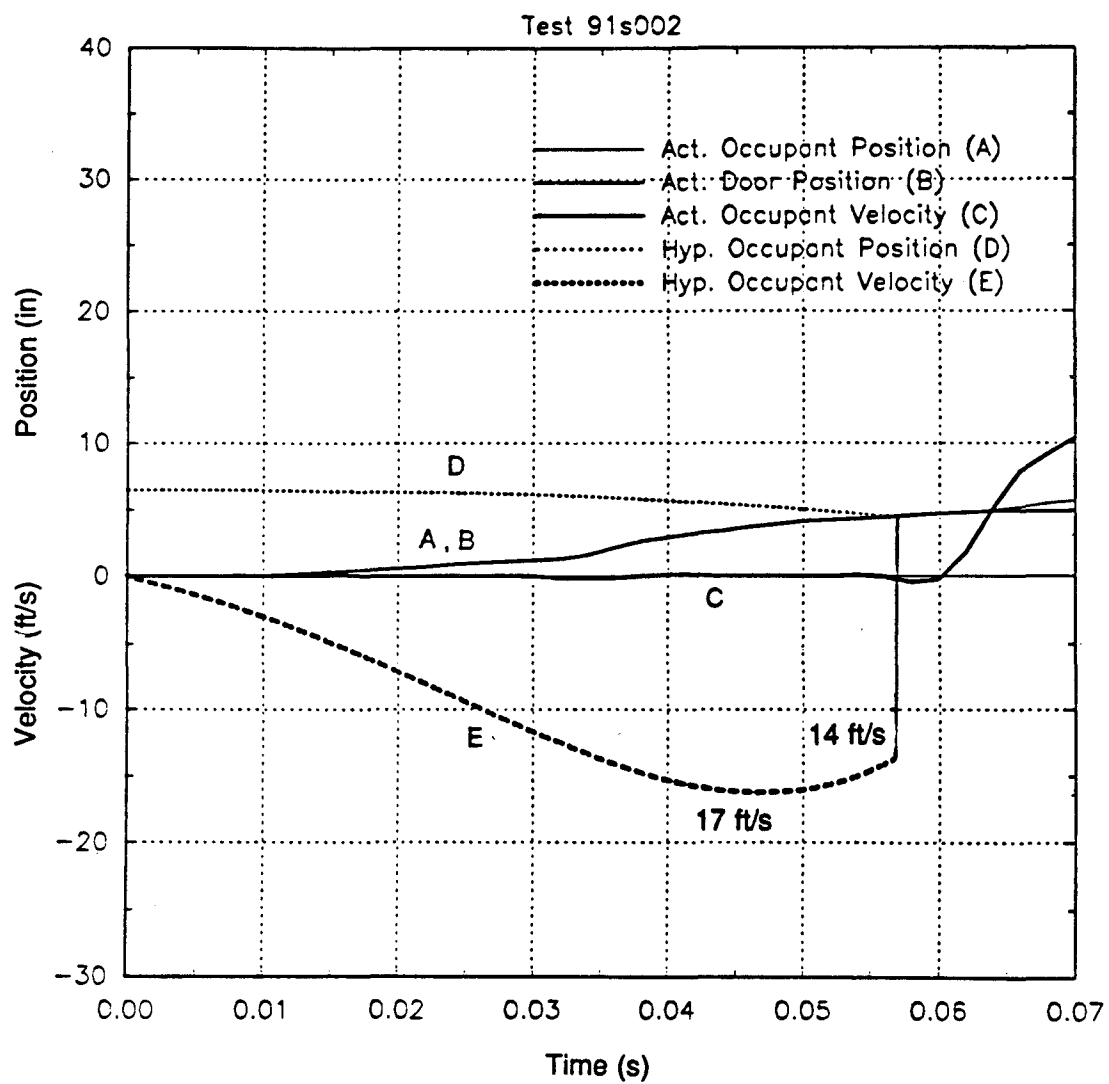
The test vehicle was a 1983 Dodge Colt and the pole was 32.8-ft (10-m) ESV luminaire support. The impact occurred at 17.8 mi/h (28.7 km/h). Upon impact the pole collapsed as designed. As the impact event progressed the vehicle started to yaw counter-clockwise, continuing forward away from the impact point. The vehicle was extensively damaged. The maximum residual crush of the vehicle at the impact point was 9 in (229 mm), the intrusion event occurred over 60 ms. The pole was extensively damaged, on impact the pole activated and began to warp around the sill and door structure. The base of the pole remained intact and did not fracture. The galvanized sheet around the base was torn in several places. Just prior to impact the dummy's head was resting against the side window of the vehicle. The ensuing direct impact from the pole to the head drove glass fragments into the skull area and the resulting HIC value of 44,101 was far in excess of the allowable limiting value of 1,000. The head of the dummy was subjected to the maximum possible impact loading in the event direct contact with pole at an impact speed equal to that of the vehicle [25.6 ft/s (7.8 m/s)]. The TTI value was as low as 47 g's.

This collision should be rated as unacceptable because of the very high HIC value. It should be noted, however, that the TTI value was quite low, and the vehicle response was stable. Figure 10 shows a graph of the positions of the occupant and the door interior during the impact event.



1 ft/s = 0.305 m/s
1 in = 25.4 mm

Figure 9. Occupant and vehicle kinematics of test 91S001.



1 ft/s = 0.305 m/s
1 in = 25.4 mm

Figure 10. Occupant and vehicle kinematics of test 91S002.

Test 91S003

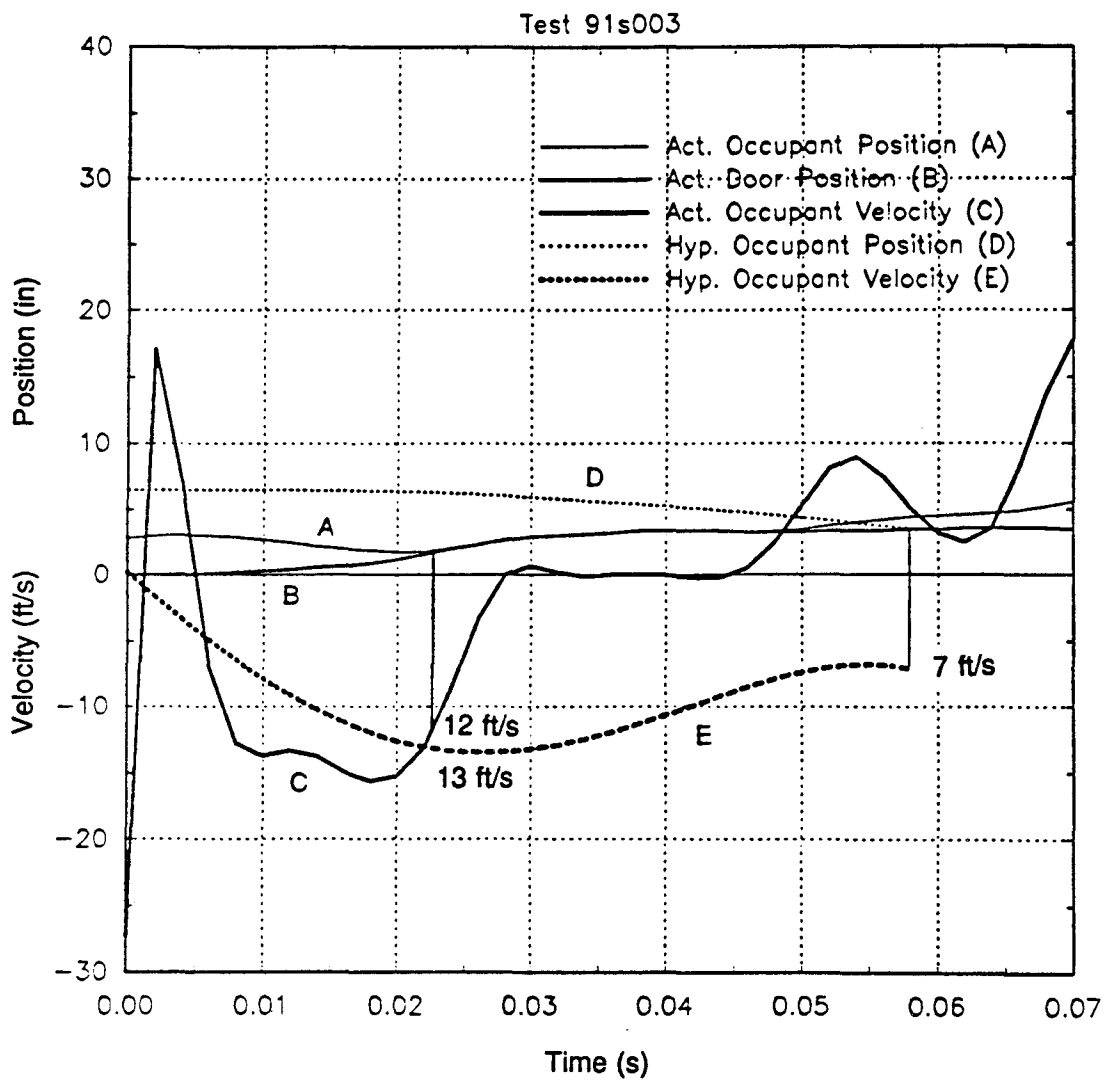
The test vehicle was a 1984 Honda Civic and the pole was a 32.8-ft (10-m) ESV luminaire support. The test vehicle impact velocity was 29.9 mi/h (48.1 km/h). The maximum residual crush of the vehicle at the impact point was 8.5 in (215.9 mm). This test was similar to test no. 91S001 except that a Honda Civic was used in place of a Dodge Colt. The door structure in the Civic is stiffer than that of the Colt, and the effect that this stiffness increase would have on the response of the ESV pole, vehicle, and vehicle occupant was of interest. Unfortunately, the ESV pole employed in this test was defective, and fracture occurred at the base of the pole. The actual impact velocity of the occupant with the interior of the vehicle was 15 ft/s (4.6 m/s). The TTI was found to be 97, which is greater than the limit of 90. The HIC observed in the test was 503, well below the usual limit of 1,000.

All occupant risk parameters in this test were within the acceptable range and the vehicle response was stable. However, the ESV pole did not perform in an energy dissipating mode as designed. Instead, the base of the pole fractured early in the impact event and the resulting dynamic response of the vehicle was similar to that typically occurs in slip-base impacts. Figure 11 shows a graph of the positions of the occupant and the door interior during the impact event.

Test 91S004

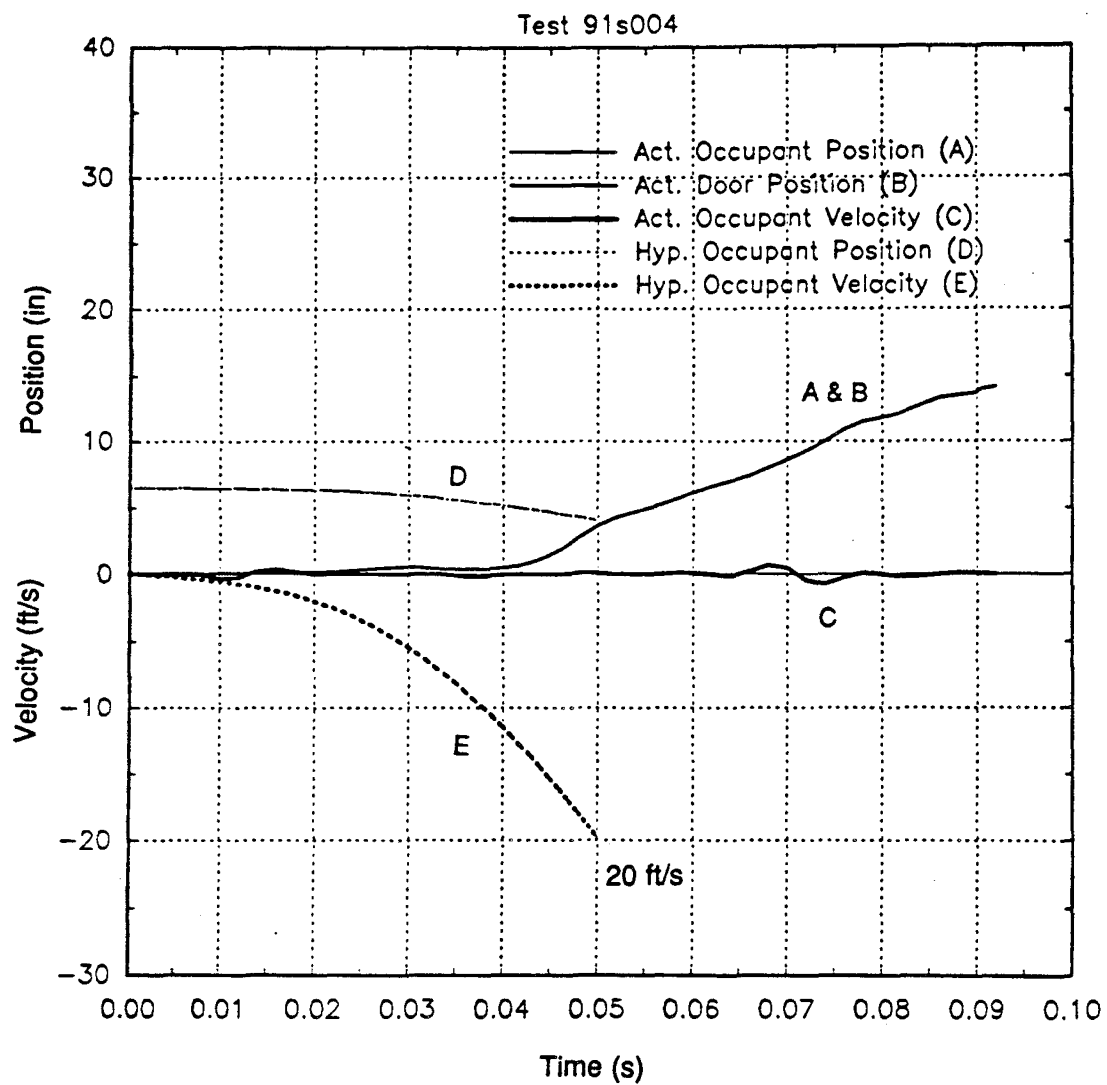
The test vehicle was a 1984 Plymouth Colt and the 30.25-ft (9.2-m) steel pole with a California type 31 slipbase. The slipbase was clamped together with three strain gauged bolts which were tightened to 14,000 lb (62 kN) each just prior to the test. The impact occurred at 18.9 mi/h (30.4 km/h). The vehicle had a maximum roll angle of 8.4 degrees as it leaned toward the test pole. The vehicle crushed inward as it slowed and stopped without breaking away the pole, thus causing a very large intrusion. The vehicle yawed slightly counter-clockwise as it came to a rest. The maximum residual crush of the vehicle at the impact point was 18.75 in (476.3 mm).

The head of the dummy was subjected to the maximum impact speed equal to that of the vehicle [26.4 ft/s (8.1 m/s)]. Figure 12 shows a graph of the positions of the occupant and the door interior during the impact event. The TTI was found to be 82, which is lower than the limit of 90. The HIC observed in the test was 2,513, higher than the usual limit of 1,000. This collision should be rated as unacceptable because of the high HIC value. It should be noted, however, that the TTI was acceptable, and the vehicle response was stable. Furthermore, all calculated occupant impact velocity values were below the limit Report 230 value of 30 ft/s (9.2 m/s).



1 ft/s = 0.305 m/s
 1 in = 25.4 mm

Figure 11. Occupant and vehicle kinematics of test 91S003.



1 ft/s = 0.305 m/s
1 in = 25.4 mm

Figure 12. Occupant and vehicle kinematics of test 91S004.

Test 91S005

The test vehicle was a 1983 Dodge Colt and the pole was a 32.8-ft (10-m) ESV luminaire support. The test vehicle impact velocity was 41.5 mi/h (66.8 km/h). Upon impact the vehicle's driver side door began to crush and the pole started to collapse. As the impact event progressed the vehicle began to yaw counter-clockwise, achieving a total yaw angle of 182 degrees. Its final resting position was approximately 22 ft (6.7 m) to the right and 10 ft (3 m) downstream of the impact point. The vehicle was extensively damaged during the collision. The maximum residual crush of the vehicle at the impact point was 10 in (254 mm). The pole was also extensively damaged. On impact the pole activated and began to wrap around the sill and door structure. Approximately 18 ft (5.5 m) of the pole was flattened and had been pulled over the sill. As the impact event progressed the inertia of the pole caused a buckle to form about 20 ft (6.1 m) up the pole. The base of the pole remained intact and did not fracture. The galvanized sheet around the base was also torn in several places. Overall the device performed in a manner consistent with its design.

Prior to impact, the dummy was in position. The actual flail distance at impact was 7 in (178 mm). The impact velocity using the flail model approach with a 1-ft (.3-m) flail distance and nondeforming passenger compartment was 17.6 ft/s (5.4 m/s), in comparison to the actual impact velocity of the occupant with the interior of the vehicle was 14 ft/s (4.3 m/s). Figure 13 shows a graph of the positions of the occupant and the door interior during the impact event.

The TTI was found to be 109 which is slightly greater than the limit of 90. The HIC observed in this test was 139, well below the usual limit of 1000.

Overall, the ESV pole performed extremely well in this high-speed test. The TTI value was moderate, the HIC was quite low, and the vehicle response was stable. Furthermore, all calculated occupant impact velocity values were below the limit Report 230 value of 30 ft/s (9.2 m/s).

Test 91S006

The test vehicle was a 1982 Dodge Colt and the pole was a 30.25 ft (9.2 m) with a California type 31 slipbase. The slipbase was clamped together with three strain gauged bolts which were tightened to 6,000 lb (26.7 kN) each prior to the test.

The test vehicle impact velocity was 20.8 mi/h (33.5 km/h). Upon impact the driver's door began to crush and the pole started to collapse. As the impact event progressed, the vehicle began to yaw counter-clockwise and continued forward away from the impact point after yawing a total of approximately 50 degrees. The final resting position was approximately 25 ft (7.6 m) to the right and 22 ft (6.7 m) downstream of the impact point.

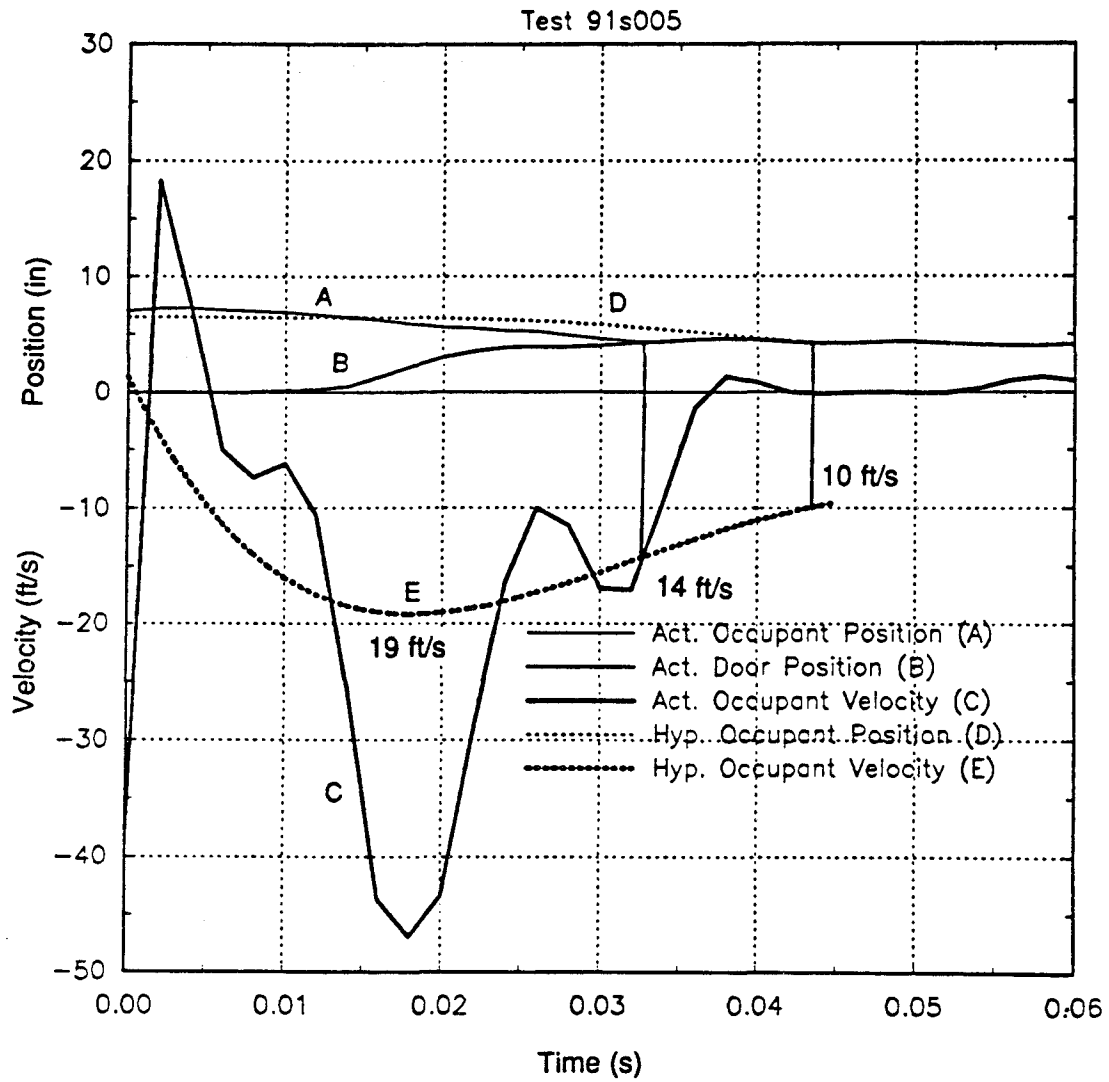


Figure 13. Occupant and vehicle kinematics of test 91S005.

The vehicle was extensively damaged during the collision. The maximum residual crush of the vehicle at the impact point was 10 in (254 mm), the pole slipped as intended, but did not suffer any additional structural damage.

Just prior to impact, the dummy was out of position, leaning in board. The actual flail distance at impact was 0 in (0 m) rather than 6.5 in (165 mm), which subjected the dummy's head to the maximum impact loading. The actual occupant impact velocity was 28.8 ft/s (8.8 m/s). The occupant impact velocity using the space flail model approach with 1-ft (.3-m) flail distance and nondeforming passenger compartment was 13.3 ft/s (4.1 m/s). A graph of the positions of the occupant and the door interior during the impact event is shown in figure 14.

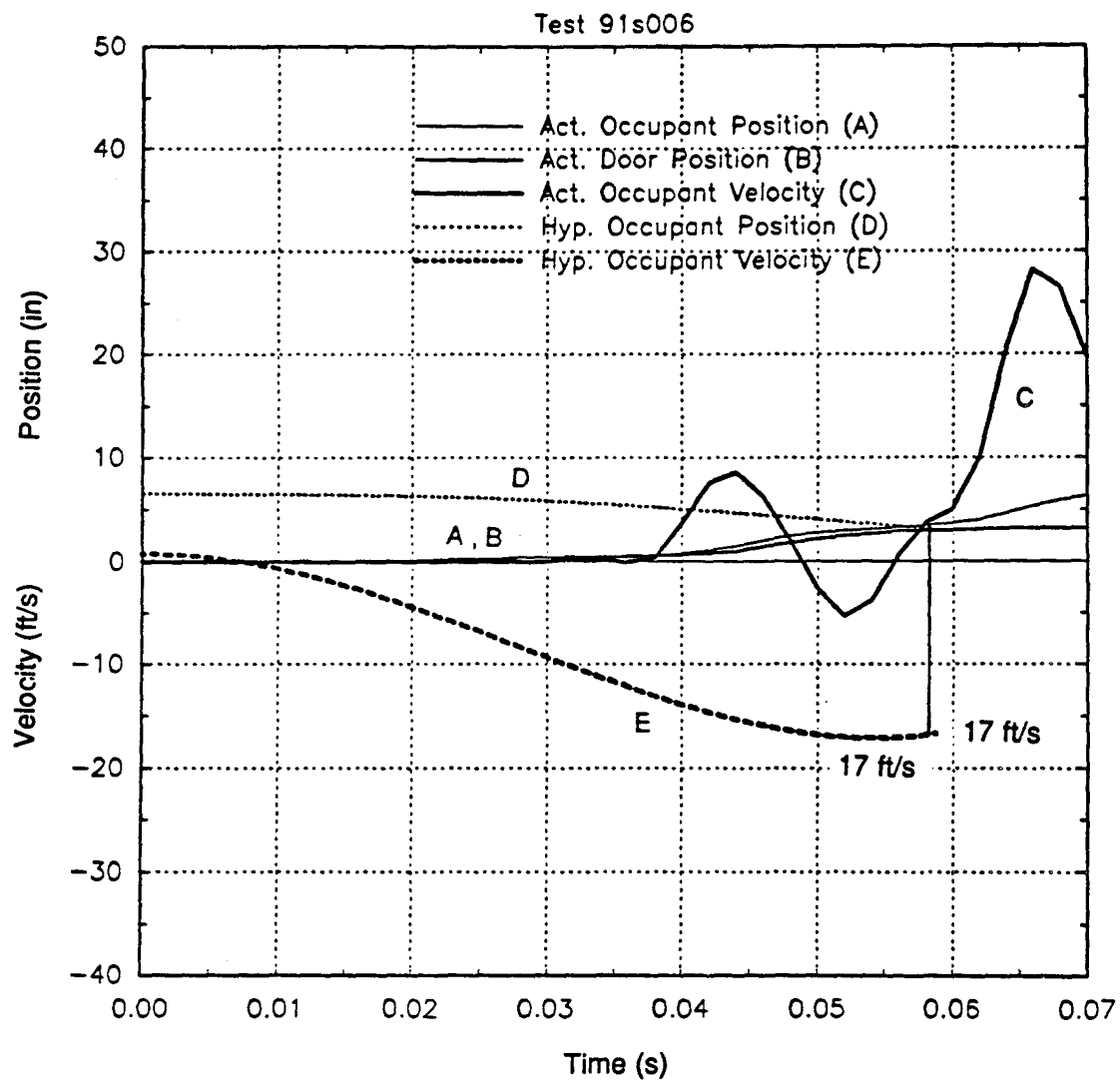
The data acquisition system associated with the side impact anthropometric dummy suffered a malfunction during this test. No dummy data was obtained and the HIC and TTI values could not be computed.

Test 91S007

The test vehicle was a 1985 Dodge Colt and the pole was a 30.25-ft (9.2-m) steel pole with California type 31 slipbase. The slipbase was clamped together with three strain gauged bolts which were tightened to 14,000 lb (62.3 kN) each just prior to the test. The test vehicle impact velocity was 39.8 mi/h (64.1 km/h). Upon impact the driver's side door began to crush and the slipbase mechanism activated. As the impact event progressed the vehicle began to yaw counter-clockwise and continued forward away from the impact point after yawing a total of 85 degrees. Its final resting position was approximately 40 ft (12.2 m) to the right and 12 ft (3.7 m) downstream of the impact point. The vehicle was extensively damaged during the collision. The maximum residual crush of the vehicle at the impact point was 13 in (330 mm). The pole released as intended, but did not suffer any structural damage.

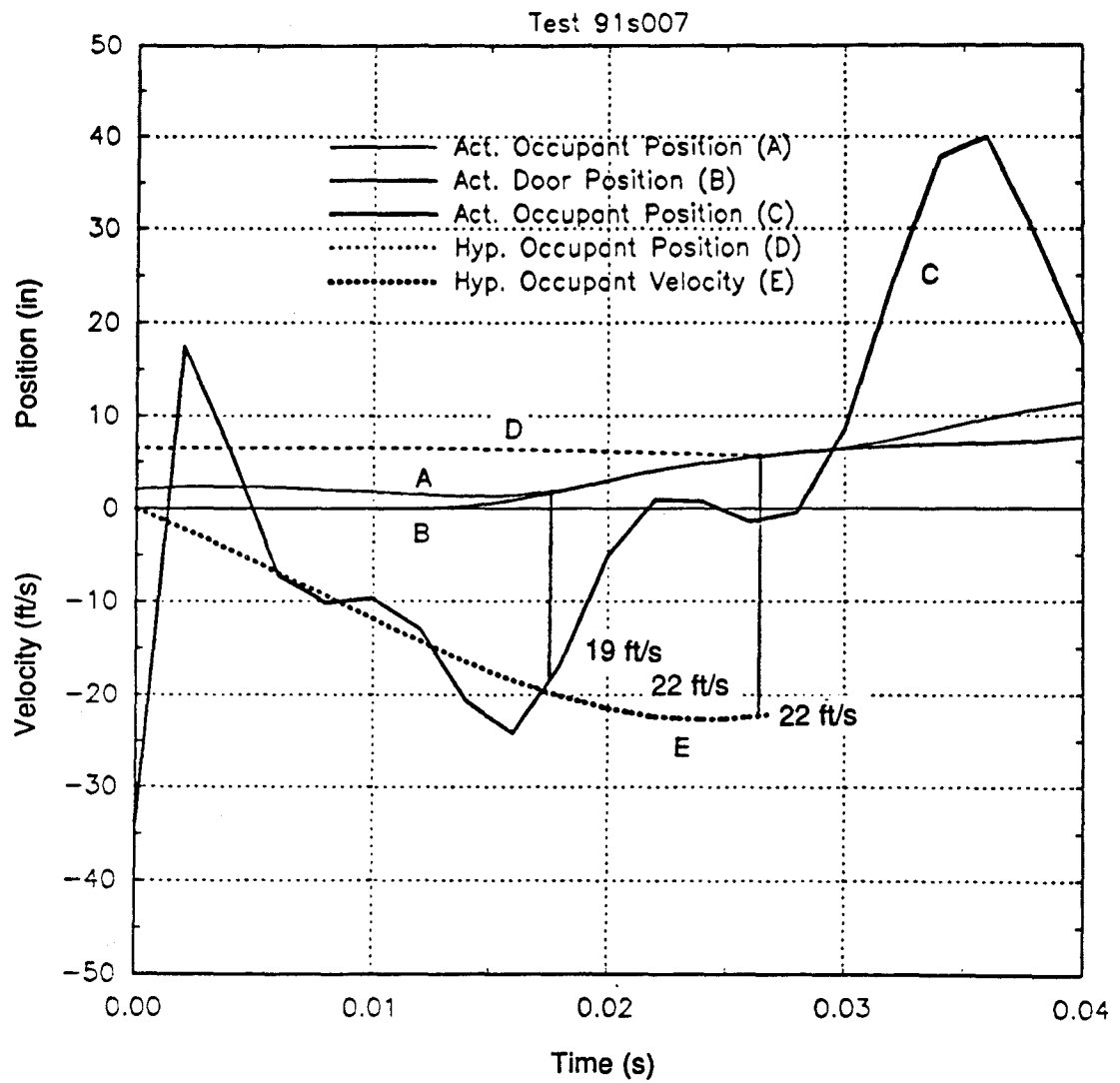
Just prior to impact, the dummy was slightly out of position, leaning in-board. The actual flail distance at impact was 2.2 in (55.9 mm) rather than 6.5 in (165 mm). After the impact the dummy rapidly accelerated toward the door, striking the window and the intruding pole. The actual occupant impact velocity was 19 ft/s (5.8 m/s), in comparison with the space flail model approach with a 1-ft (.3-m) flail distance and nondeforming passenger compartment was 11.11 ft/s (3.4 m/s). A graph of the positions of the occupant and the door interior during the impact event is shown in figure 15. The TTI was found to be 413, which is much greater than the limit of 90. The HIC observed in the test was 17,776 well above the used limit of 1,000.

This collision should be rated as unacceptable because of the extremely high HIC and TTI. Fatal injuries would probably have resulted from this impact. The calculated occupant risk parameters were well within acceptable Report 230 limits.



1 ft/s = 0.305 m/s
1 in = 25.4 mm

Figure 14. Occupant and vehicle kinematics of test 91S006.



1 ft/s = 0.305 m/s
1 in = 25.4 mm

Figure 15. Occupant and vehicle kinematics of test 91S007.

Test 91S036

This test investigated the impact performance of a standard BCT in a side impact collision with a 1985 Honda Civic Si. The BCT was developed in the early 1970's to provide a safe method for terminating guardrails.^[20] In an end-on collision, the BCT posts are designed to fracture allowing the W-beam to buckle. The vehicle is impulsively directed either in front of or behind the barrier. This process is often called "gating." The terminal is also designed so that it provides the required anchorage for impacts downstream from the end. The BCT must be strong enough to serve as an anchor in mid-length collisions while breaking away in end-on collisions. The test vehicle impact velocity was 31 mi/h (49.9 km/h) and the impact point was near the center of the driver-side door. On impact the nose element of the BCT was crushed against the first post of the system. The first post did not break, and the breakaway mechanism did not activate. The only significant damage to the BCT was the deformation of the nose element. The vehicle damage was extensive. The maximum intrusion into the passenger compartment was 39 in (991 mm).

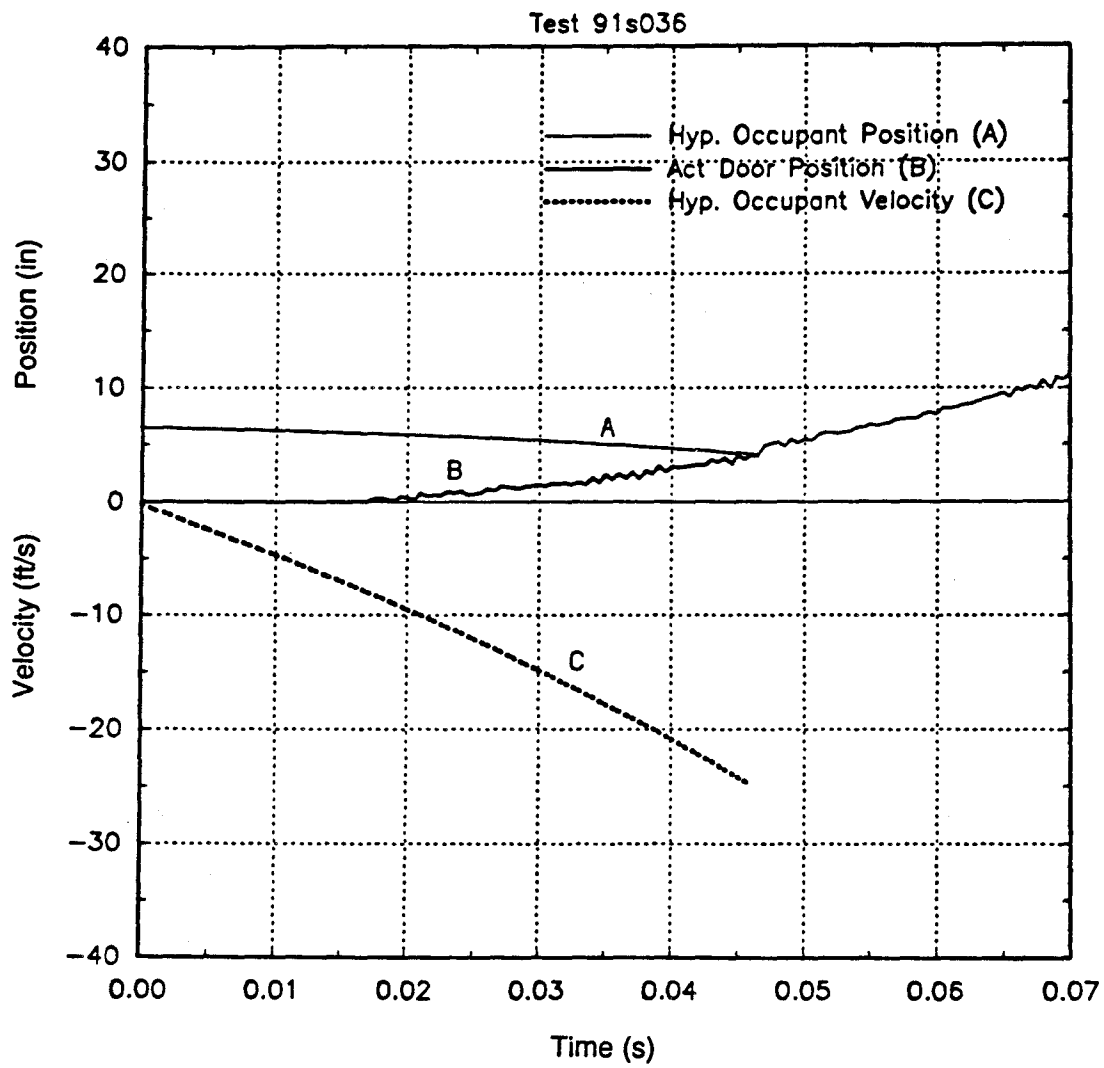
Vehicle acceleration data was processed to determine the impact velocity of a hypothetical front seat passenger against the vehicle interior in accordance with the flail space model recommended in *National Cooperative Highway Research Program (NCHRP) Report 230*.^[3] The lateral impact velocity of the hypothetical occupant using the flail space model approach with a 1-ft (0.3-m) flail distance and a nondeforming passenger compartment (i.e., the usual flail space model) was 23.9 ft/s (7.3 m/s). The lateral impact velocity design limit specified for lateral impacts with highway safety appurtenances in *NCHRP Report 230* is 20 ft/s (6.1 m/s). An analysis of the occupant impact velocity that includes the effect of the interior of the door moving into the occupant compartment was also performed. The impact velocity of the occupant with the interior of the vehicle based on an analysis of a displacement transducer placed inside the vehicle was 25.3 ft/s (7.7 m/s). The breakaway cable terminal was chosen because it is a common guardrail terminal used throughout the United States. This test is believed to be the first side impact crash test of a guardrail terminal.

A summary of the test conditions and results for this full-scale crash test are given in table 5 and the hypothetical occupant and vehicle kinematic histories are presented in figure 16. This collision is rated as unacceptable primarily because of the extensive vehicle damage and high probability that an occupant in such a collision would have been fatally injured.

Table 5. Summary of the terminal test conditions and results.

FOIL test no.	91S036	91S037	91S038	91S046
Structure	BCT	ELT	MELT	MELT-SI
Test vehicle year [Honda Civic Si]	1985	1984	1984	1984
Vehicle weight, test inertial (lb)	1,850	1,850	1,850	1,850
Vehicle weight, gross static (lb)	2,015	1,850	2,015	1,850
Number of occupants	none	none	none	none
Soil type (strong)	S1	S1	S1	S1
Soil condition	Dry	Dry	Dry	Dry
Impact speed-nominal (mi/h)	30.0	30.0	30.0	30.0
Impact speed-actual (mi/h)	31.0	31.8	28.4	29.5
Impact point, observed	Driver-side door (17 in behind cg) (24 in in front of B pillar)	Driver-side door (17 in behind cg) (24 in in front of B pillar)	Driver-side door (17 in behind cg) (24 in in front of B pillar)	Driver-side door (17 in behind cg) (24 in in front of B pillar)
Vehicle Damage				
Traffic accident data	9-LP-7	9-LP-7	9-LP-7	9-LP-6
Vehicle Damage Index	09LDAW7	09LDAW7	09LDAW7	09LDAW4
Maximum vehicle crush (in)	39	30	37.3	14
Area crushed (in ²)	1,124	1,207	1,152	524
Maximum static intrusion (in)	29.9	29.9	31.5	11
Intrusion rate (in/s)	340	366	323	217
Occupant impact velocities				
Design limit (<i>Report 230</i>) (ft/s)	20	20	20	20
Allowable limit (<i>Report 230</i>) (ft/s)	30	30	30	30
Calculated for 12 in flail space (ft/s)	23.9	25.7	23.9	21.1
Impact time (12 in flail) (s)	0.094	0.080	0.094	0.086
Calculated for 6.5 in flail space (ft/s)	17.7	19.1	17.7	15.8
Impact time (6.5 in flail) (s)	0.073	0.060	0.073	0.061
Normalized impact velocity (ft/s)	25.3	38.0	25.3	26.0
Normalized impact time (s)	0.047	0.043	0.047	0.044
Hypothetical occupant ridedown accelerations				
Design limit (<i>Report 230</i>)	15 g's	15 g's	15 g's	15 g's
Allowable limit (<i>Report 230</i>)	20 g's	20 g's	20 g's	20 g's
Calculated for 6.5 in flail space	21.4 g's	18.2 g's	21.4 g's	14.4 g's
Calculated for 12 in flail space	21.4 g's	14.7 g's	21.4 g's	11.3 g's
Hypothetical Thoracic Trauma				
Thoracic Trauma Index	117 g's	120 g's	103 g's	37 g's
Probability of AIS > 3 injury	0.79	0.81	0.66	0

1 lb = 4.448 N = 0.45 kg
 1 in = 25.4 mm
 1 mi/h = 1.61 km/h
 1 ft/s = 0.305 m/s



1 in = 25.4 mm
1 ft/s = 0.305 m/s

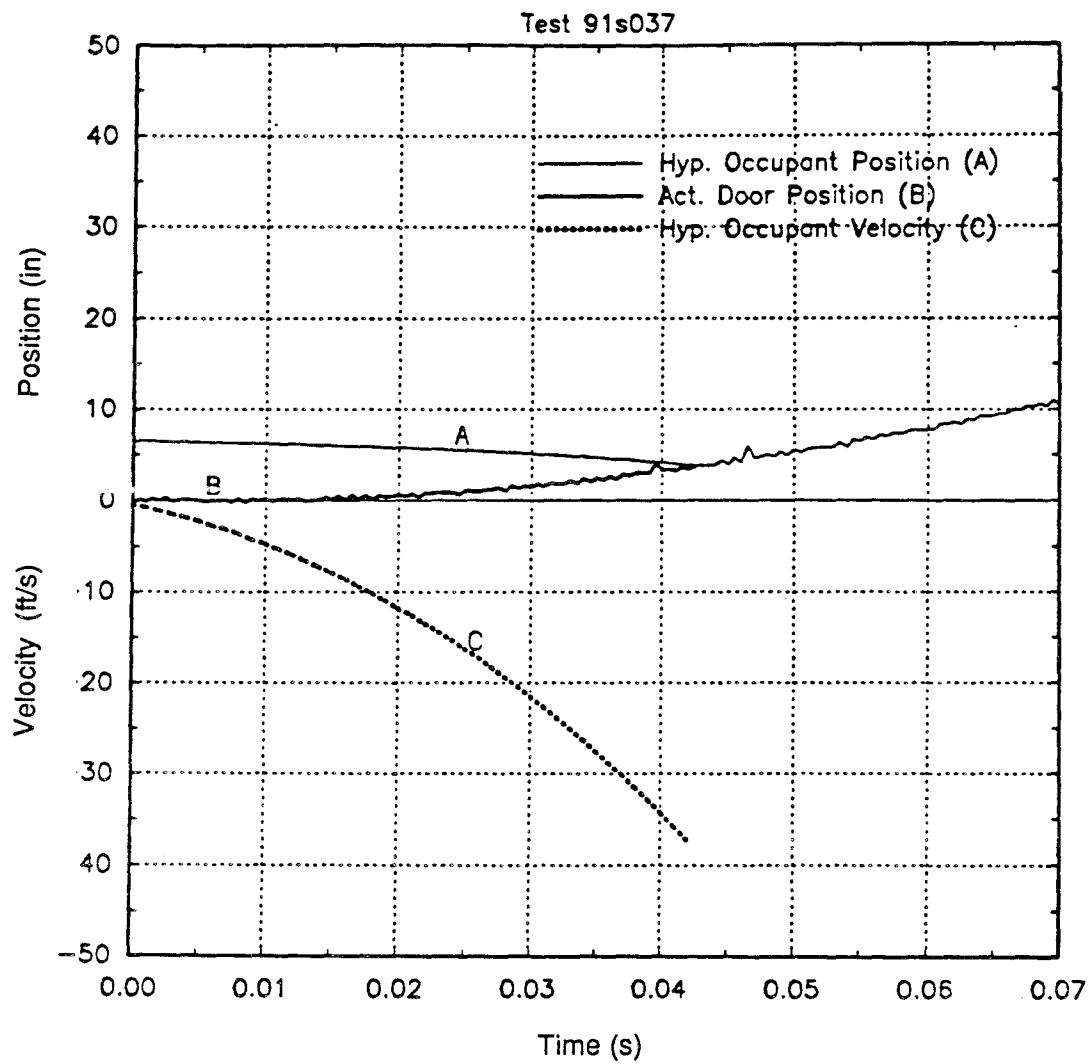
Figure 16. Occupant and vehicle kinematics of test 91S036.

Test 91S037

This test investigated the impact performance of a standard ELT in a collision with a 1984 Honda Civic Si. The nose piece of the BCT was replaced with a culvert section containing a loader arm. When hit head-on this loader arm introduces a buckling load into the W-beam. The W-beam is not bolted to the rail in the first 25 ft (7.6 m) of guardrail so the beam is essentially unsupported once the first post breaks. The large unsupported length makes the buckling load for the W-beam very low. This low buckling load minimizes the resistance to the striking vehicle. The post placement is slight different than the placement used in the BCT. A sharper parabolic curve is used to further enhance the buckling action of the W-beam. The usual BCT anchor cable is included to provide a tensile reaction in downstream collisions. A spreader bar is located between the first and second posts to distribute the downstream foundation load over the first two posts. The test vehicle impact velocity was 31.8 mi/h (51.2 km/h) and the impact point was near the center of the driver-side door. On impact the nose element of the ELT was pushed into the driver side door with little deformation of the ELT nose. The unbolted portion of the beam buckled out but did not fall off the shelf bracket. The first post split vertically but did not break away. The nose of the unit was deformed and some tears were observed in the corrugated culvert section, but the nose assemble retained its original cylindrical shape. Other than the split post and deformation of the culvert section, there was little damage to the ELT. Vehicle damage was extensive. The maximum intrusion into the passenger compartment was almost 28 in (711 mm).

Vehicle acceleration data was processed to determine the impact velocity of a hypothetical front seat passenger against the vehicle interior. The lateral impact velocity of the hypothetical occupant using the flail space model approach with a 1-ft (0.3-m) flail distance and a nondeforming passenger compartment (i.e., the usual flail space model) was 25.7 ft/s (7.8 m/s). The lateral impact velocity design limit specified for lateral impacts with highway safety appurtenances in *NCHRP Report 230* is 20 ft/s (6.1 m/s). An analysis of the occupant impact velocity that includes the effect of the interior of the door moving into the occupant compartment was also performed. The impact velocity of the occupant with the interior of the vehicle based on an analysis of a displacement transducer placed inside the vehicle was 38 ft/s (11.6 m/s).

A summary of the test conditions and results for this full-scale crash test are given in table 5 and the hypothetical occupant and vehicle kinematic histories are presented in figure 17. This collision is rated as unacceptable primarily because of the extensive vehicle damage and high probability that an occupant in such a collision would have been fatally injured. Specifically the hypothetical occupant impact velocity was well above the absolute limit.



1 in = 25.4 mm
1 ft/s = 0.305 m/s

Figure 17. Occupant and vehicle kinematics of test 91S037.

Test 91S038

This test investigated the impact performance of a MELT in a collision with 1985 Honda Civic Si. The MELT is the latest variation of the breakaway cable terminal family of W-beam guardrail end treatments. The MELT borrows some of the features of the ELT like a sharper parabolic flare and a laterally unsupported W-beam section near the end of the terminal. The nose element is similar to the BCT nose except horizontal baffle plates are added to stiffen the nose element and provide a moment arm that will buckle the laterally unsupported W-beam. In an end-on collision, the first two posts fracture allowing the W-beam to buckle. The vehicle is impulsively directed either in front of or behind the barrier. This process is called "gating." The terminal is also designed so that it provides the required anchorage for impacts downstream from the end. The MELT must be strong enough to serve as an anchor in mid-length collisions while breaking away in end-on collisions. The test vehicle impact velocity was 28.4 mi/h (45.7 km/h) and the impact point was near the center of the driver-side door. On impact the nose element of the MELT began intruding into the vehicle's passenger compartment. The first post did not break and the breakaway mechanism did not activate. The only significant damage to the MELT was the deformation of the nose element. The vehicle damage was extensive. The maximum intrusion into the passenger compartment was almost 32 in (813 mm).

Vehicle acceleration data was processed to determine the impact velocity of a hypothetical front seat passenger against the vehicle interior in accordance with the flail space model. The lateral impact velocity of the hypothetical occupant using the flail space model approach with a 1-ft (0.3-m) flail distance and a nondeforming passenger compartment (i.e., the usual flail space model) was 23.9 ft/s (7.3 m/s). The lateral impact velocity design limit specified for lateral impacts with highway safety appurtenances in *NCHRP Report 230* is 20 ft/s (6.1 m/s). An analysis of the occupant impact velocity that included the effect of the interior of the door moving into the occupant compartment was also performed. The impact velocity of the occupant with the interior of the vehicle based on an analysis of a displacement transducer placed inside the vehicle was 25.3 ft/s (7.7 m/s).

A summary of the test conditions and results for this full-scale crash test are given in table 5 and the hypothetical occupant and vehicle kinematic histories are presented in figure 18. This collision is rated as unacceptable primarily because of the extensive vehicle damage and high probability that an occupant in such a collision would have been fatally injured.

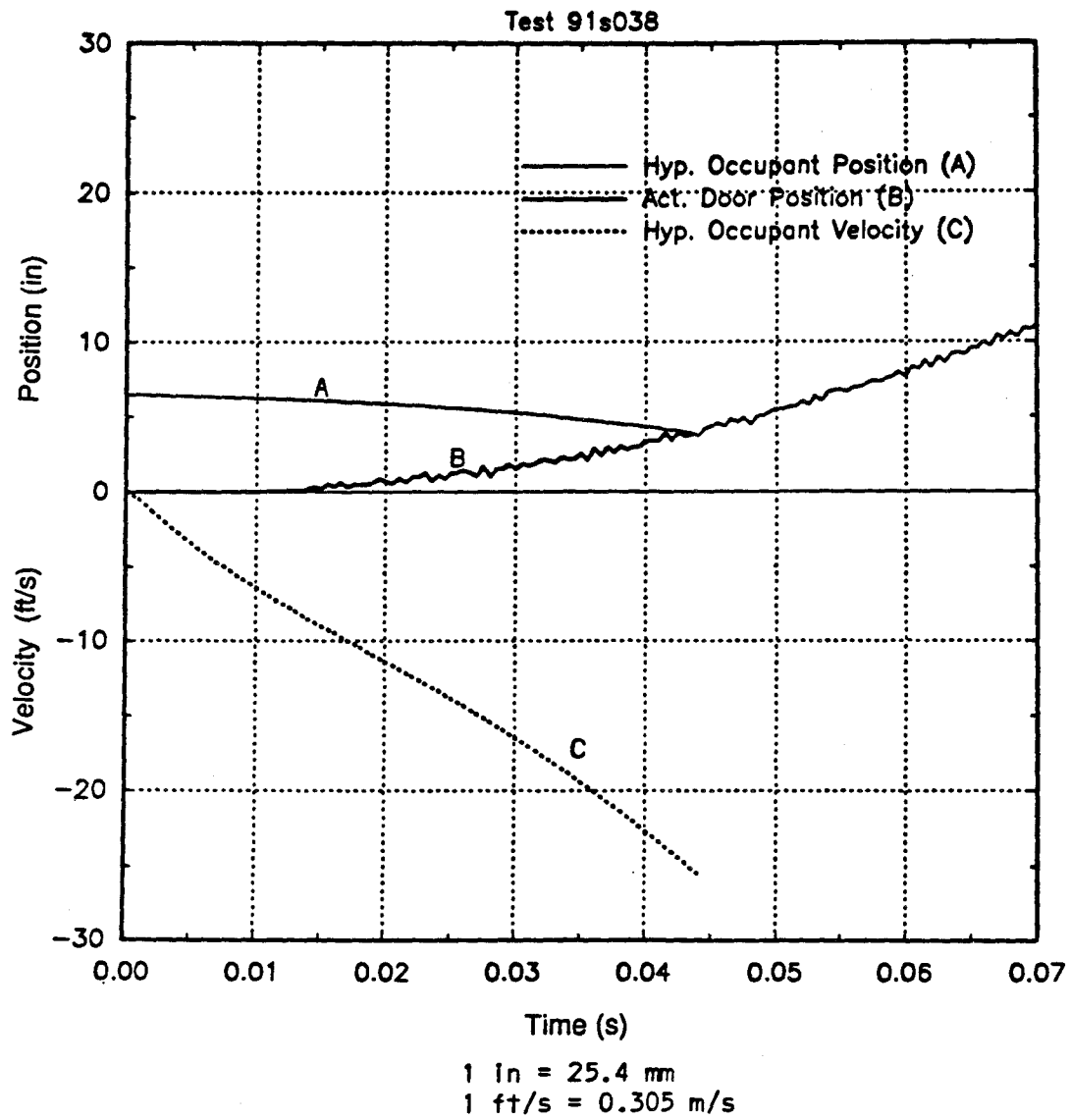


Figure 18. Occupant and vehicle kinematics of test 91S038.

Test 91S046

This test investigated the impact performance of a MELT-SI in a collision with 1985 Honda Civic Si. This enhanced version of the MELT was specifically designed to activate in a side impact collision. The MELT is an improved version of the BCT and the ELT. The design details of the enhanced MELT are presented in Test Report FHWA-RD-92-052. The test vehicle impact velocity was 29.5 mi/h (47.5 km/h) and the impact point was near the center of the driver-side door. On impact the nose element of the MELT-SI began to crush the driver side door. The lower skirt on the nose contacted the lower sill of the vehicle very soon after the initial impact. The first post of the system fractured allowing the unsupported W-beam to buckle. The vehicle continued to travel sideways until it contacted the second post. The second post also fractured and the vehicle came to rest in contact with the second post. The MELT-SI was significantly damaged and would not have been effective as either an anchor or terminal in a subsequent collision. The nose element was deformed, the first section of W-beam was buckled and the first two posts of the system were fractured. The vehicle damage was extensive but much less severe than in either of the three preceding tests. The maximum intrusion into the passenger compartment was 11 in (279 mm).

Vehicle acceleration data was processed to determine the impact velocity of a hypothetical front seat passenger against the vehicle interior in accordance with the flail space model. The lateral impact velocity of the hypothetical occupant using the flail space model approach with a 1-ft (0.3-m) flail distance and a nondeforming passenger compartment (i.e., the usual flail space model) was 21.1 ft/s (6.4 m/s). The lateral impact velocity design limit specified for lateral impacts with highway safety appurtenances in *NCHRP Report 230* is 20 ft/s (6.1 m/s). An analysis of the occupant impact velocity that includes the effect of the interior of the door moving into the occupant compartment was also performed. The impact velocity of the occupant with the interior of the vehicle based on an analysis of a displacement transducer placed inside the vehicle was 26.0 ft/s (7.9 m/s).

A summary of the test conditions and results for this full-scale crash test are given in table 5 and the hypothetical occupant and vehicle kinematic histories are presented in figure 19. The breakaway mechanism performed as intended and the risk of severe or fatal injury to vehicle occupants as measured by both the thoracic trauma index and the occupant risk criteria were below the suggested limits of 100 g's and 30 ft/s (9.2 m/s). The test is considered acceptable.

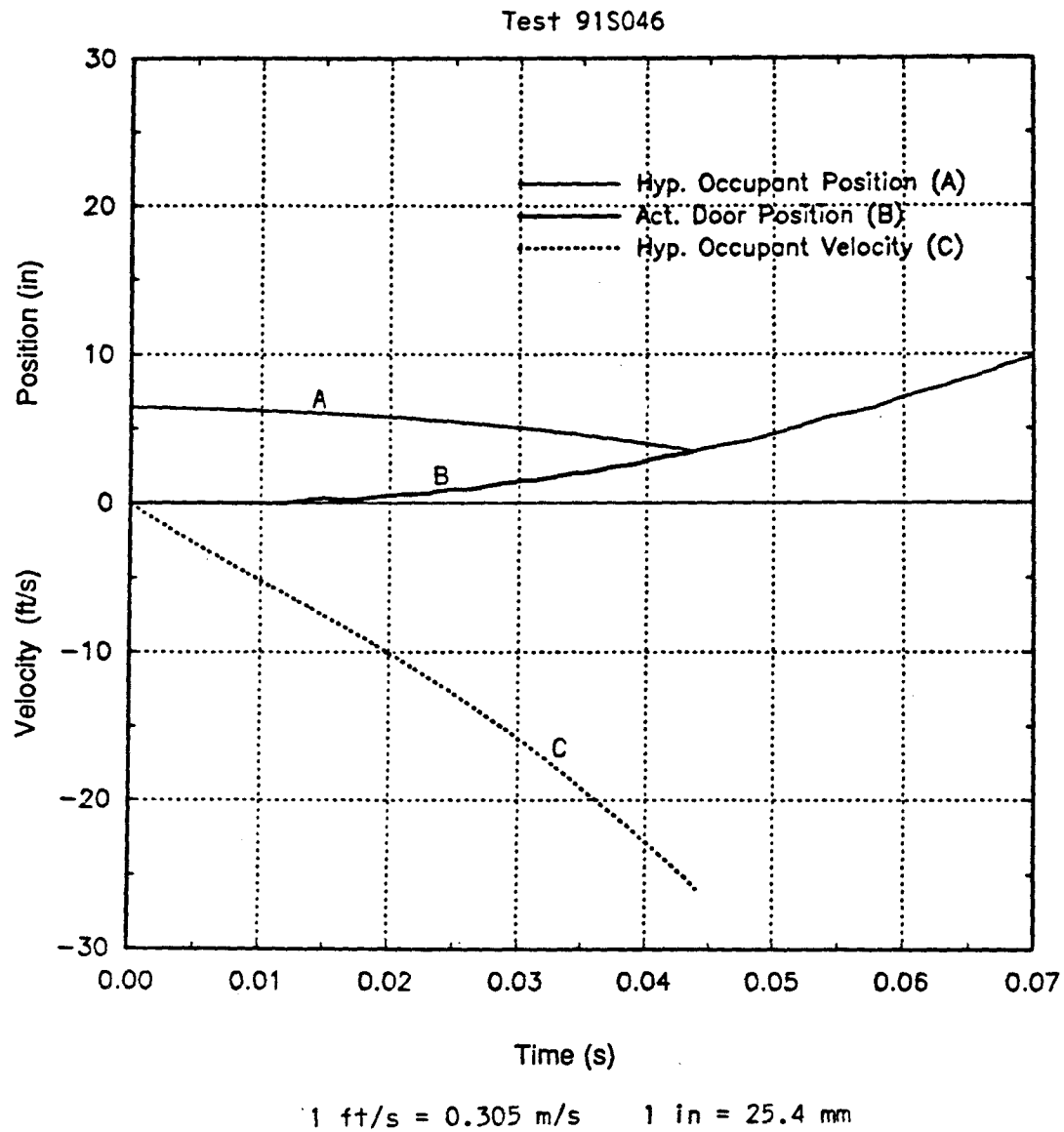


Figure 19. Occupant and vehicle kinematics of test 91S046.

Chapter 4. Severity Modelling

Introduction

Crash tests are the best method of evaluating the performance of roadside hardware. Full-scale tests subject the test articles to realistic impact loads that are difficult to estimate or simulate. Successful performance in a crash test demonstrates the dynamic capabilities of a structure.

Although test performance is important, the success of a roadside structure must eventually be established in the field. The ultimate performance measure for a roadside device is the probability of an occupant in a similar collision escaping serious injury. The objective of all roadside hardware is to shield the occupant from injury-producing events. Unfortunately, measuring the chance of serious injury in a real-world accident using crash tests is a difficult task.

The current specifications on full-scale appurtenance crash testing, *NCHRP Report 230* present several evaluation parameters that are used to judge the hypothetical risk to vehicle occupants.^[3] For example, rollover is known to be a very hazardous event in a collision.^[24] Rollovers are usually unacceptable because they nearly always produce an unacceptably high chance of serious injury. The occupant risk criteria is another attempt to rate the risk to vehicle occupants based on the hypothetical impact velocity between the occupant and the vehicle interior and the maximum 10 ms average acceleration after the occupant has contacted the interior. The relationship between the occupant risk criteria and the actual risk of real occupants has never been firmly established, especially for lateral head impacts. There is very little linkage between the *Report 230* limits and biomechanics research.

The automotive design and regulatory community has also developed a number of evaluation criteria. Automotive biomechanics criteria have been based on the response of anthropometric dummies in full-scale crash tests. These dummy responses have, to varying degrees, been related to the risk of human injury using cadaver and animal testing. While the design of dummies and analysis methods has continued to be a vigorous area of research, there are much better connections between the response of anthropometric devices and real human injury. These linkages will be discussed in the following section.

Traditionally the roadside design community has preferred not to use dummy-based evaluation criteria. The environment in many full-scale crash tests of roadside safety appurtenances is so severe it is often not advisable to place dummies in the vehicle. Good dummy results require careful and frequent calibration which has traditionally been a problem for roadside safety applications. Since the response of the vehicle can be easily measured in a full-scale test, vehicle-based evaluation parameters that estimate the response of hypothetical humans have been preferable to the use of fully instrumented anthropometric dummies. There are several reasons for testing without dummies:

(1) dummies are expensive to acquire and calibrate and (2) many appurtenance crash tests are too severe to risk damaging an anthropometric dummy. In the past, the value of using instrumented dummies was not deemed sufficient compared to the cost of acquiring, calibrating and using them.

Regardless of reasons for not using dummies in appurtenance crash tests in the past, the best connection to human tolerance research is through the use of anthropometric dummies. For this reason, using anthropometric dummies in side impact appurtenance crash tests for the foreseeable future is probably unavoidable. Vehicle-based (non-dummy) performance criteria could be developed by relating observable test results to the observed dummy responses. As the number and variety of tests increases, mathematical models of human risk could be developed. When there is sufficient statistical confidence in the models, dummies could be removed from the test vehicles.

There are several advantages to this approach. First, removal of dummies makes the tests less expensive to perform and evaluate. Second, tests that are based only on observed dynamics of the vehicle will be more repeatable than tests involving dummies. The response of a dummy in a test is subject to numerous small, uncontrollable and sometimes unobservable subevents within the collision. While these subevents doubtless cause injury in real accidents, they should not be used to characterize the performance of the roadside hardware. Most of these subevents are related to the vehicle's design: the location of arm rests, the characteristics of padding, the stiffness of the A-pillar and so forth. Lastly, the process of developing models forces the research to postulate about the cause and effect relationships between the response of the vehicle and the response of the dummy. Even a partial understanding of the parameters that affect injury mechanisms can help hardware designers to build better roadside appurtenances. While it is overly optimistic to presume that a complete understanding of the injury process in side impact collisions can be attained, this model development can result in a reduction of occupant trauma in this type of collision.

Modelling Process

The following section describes the process of building preliminary vehicle-based, transformer-based evaluation criteria. These criteria are based on the results of only 15 tests of slip-base and collapsing poles so they should be viewed as first-order estimates. The addition of more test data should allow for the creation of better evaluation criteria.

Regression models that predict the TTI and HIC were developed to explore this approach to formulating evaluation criteria. Fully instrumented side impact dummies were used in all the side impact crash tests shown in table 6 so the HIC and TTI were available.

Table 6. Side impact crash test parameters.

Test no.	TTI g's	HIC	r in	V_i ft/s	V_{occ} ft/s	s in	c_e ft	a_{rd} g's	\dot{c}_i ft/s	C_{area} in ²
91s001	145	398	0	43.8	15	11.5	1.33	4.4	22.5	252
91s002	47	44,101	0	26.1	26	0.0	0.75	2.3	12.5	170
91s003	97	503	0	43.9	12	3.0	0.71	2.4	11.8	191
91s004	82	2,513	0	27.7	26	0.0	1.56	11.6	17.4	350
91s005	109	139	0	60.8	14	7.0	0.83	6.7	23.8	258
91s007	413	17,776	0	58.3	18	2.0	1.08	5.5	27.0	271
1785-2	291	3,385	0	42.0	33	4.7	2.17	8.3	15.7	780
1785-3	224	8,684	0	44.7	10	2.1	0.79	2.3	10.1	263
1785-4	192	8,026	0	44.0	13	2.4	0.83	1.5	10.6	242
1785-5	58	64	12	43.5	17	1.9	1.08	3.1	13.8	250
1785-6	126	2,191	12	41.4	14	5.2	3.00	4.9	19.2	942
1785-7	14	150	24	42.3	12	3.3	0.64	3.5	4.3	228
1785-8	91	1,996	0	43.4	18	4.0	0.63	2.0	8.0	211
1469-4	217	2,827	0	42.8	24	3.8	0.88	3.7	12.1	250
1469-6	233	9,307	0	44.1	19	4.2	1.43	1.4	16.0	385

1 in = 25.40 mm

1 ft = 0.3048 m

1 ft/s = 0.3048 m/s

1 mi/h = 1.6079 km/h

The parameters collected in the tests and used in modelling the TTI and HIC are:

r	The longitudinal distance between the occupant and the impact point in inches.
s	The actual lateral flail distance between the dummy's head and the interior of the vehicle. This distance is measured at the elevation of the dummy's ear in inches.
V_i	The lateral velocity of the vehicle at the moment of contact with the test device in ft/s. The longitudinal velocity in the tests were essentially zero.
V_{occ}	The actual velocity that the dummy strikes the intruding door in ft/s. This is not the flail space occupant impact velocity. It is based on the onboard film analysis.
c_e	The maximum external static crush of the vehicle in inches.
a_{rd}	The 10-ms average occupant ridedown acceleration in g's.
\dot{c}_i	The average velocity of the inner door surface into the passenger compartment in ft/s. This was estimated by dividing the maximum static intrusion by the length of time required for the intrusion event. This was measured directly with a string pot transducer in the four side impact tests of guardrail terminals and using film analysis in the pole tests.
C_{area}	The damaged area of the vehicle in square inches evaluated by calculating the planar horizontal area crushed on the vehicle using the six-point NHTSA sketches. The six depth measurements were taken on the moulding line of the vehicle.
TTI	The thoracic trauma index (TTI), as defined in the final rules on FMVSS 214, is the average of the maximum rib and spinal accelerations. ^[5]
HIC	The head injury criteria (HIC) is a measure of head trauma during an impact. It should be computed as specified in FMVSS 208. ^[25]

The symbols shown above will be used throughout the rest of this report to denote these values. The equations presented in the next sections were derived in Imperial units so values should be converted from SI units to imperial units prior to calculating the expected values.

Determining the form of the regression equation is one of the most difficult parts of the model building process. Selecting a form involves making assumptions about how parameters are related to each other. Several forms were evaluated in building models of HIC and TTI.

Linear Forms: The simplest type of regression is a least squares line relating the independent and dependent variables. Given a set of experimental observations of the X_{ij} and Y_j , values for the β_i can be determined that minimize the sum of the squared errors. The resulting equation is the best fit for this particular form where the subscript j represents each individual observation. The simple linear form is given by:

$$Y_j = \beta_0 + \sum_{i=1}^n \beta_i X_{ij} + \epsilon_j \quad (8)$$

Each ϵ_j is the residual error in the j th observation. This type of model is appropriate when a quantity is dependent on additive contributions from several independent sources like three drain pipes filling a retention pond. This form was not thought to be appropriate for predicting dummy response because neither the HIC nor TTI is the sum of independent effects. Intuitively, dummy response should be a combination of effects that are multiplicative rather than additive. Additive models were examined briefly but abandoned because they produced low R^2 s and were not intrinsically appealing.

Least-squares relationships between TTI and HIC and a variety of observable test parameters were found in an earlier project.^[15] The coefficients of regression (R^2) for the predictions of TTI and HIC were usually below 0.10 with one exception. Regressions were also performed to predict the occupant impact velocity with the vehicle interior. Parameters like static residual crush and vehicle speed reduction were good predictors of occupant impact velocity, having R^2 greater than 0.85.

Log-linear Exponent Forms: Using the assumption that independent effects have a multiplicative relationship leads to log-linear models. One alternative form is to assume that each independent parameter is a power of an unknown value. This results in the following form:

$$Y_j = \beta_0 \prod_{i=1}^n \beta_i^{X_{ij}} + \epsilon_j$$

Taking the natural logarithm of each side of this expression yields the following linear equation:

$$\ln(Y_j) = \ln(\beta_0) + \sum_{i=1}^n X_{ij} \ln(\beta_i) + \epsilon_j \quad (9)$$

A simple multiple linear regression can be performed using this form where the dependent variable is the natural logarithm of the observed Y_j . The values of $\ln(\beta_i)$ are found using a linear regression procedure.

Log-linear Parameter Forms: Another log-linear form could be developed by raising the independent parameters (X_{ij}) to unknown powers (β_i).

$$Y_j = \exp(\beta_0) \prod_{i=1}^n X_{ij}^{\beta_i} + \epsilon_j$$

Again, the natural logarithm of each side is taken resulting in the following linear expression.

$$\ln(Y_j) = \beta_0 + \sum_{i=1}^n \beta_i \ln(X_{ij}) + \epsilon_j \quad (10)$$

The unknown values of β_i can be found using a simple multiple linear regression and the resulting values can be resubstituted into the original equation.

Log-linear Mixed Parameter Forms: Mixing the parameter and exponential forms was also used to develop models. This form provides flexibility in assigning the type of functional relationship between a particular independent variable and the dependent variable.

$$Y_j = \exp(\beta_0) \left\{ \prod_{i=1}^n X_{ij}^{\beta_i} \right\} \left\{ \prod_{i=n}^m \beta_i^{X_{ij}} \right\} + \epsilon_j \quad (11)$$

Evaluating Regression Models: There are many possible regression models that could be evaluated. Given a particular model form, there are many different potential models available depending on the set of independent parameters (X_{ij}) chosen for the right-hand side of the equation. There are several measures that can be used to compare regression models: the coefficient of regression (R^2) and the adjusted coefficient of regression (R_a^2).^{[26],[27]} R^2 is a measure of how much information is present in the model and how much appears to be random error. A high R^2 suggests that the model explains much of the phenomena; a low R^2 suggests that the model is not an effective predictor. Since regression is a least-squares process, there should be more data than independent parameters. If there are four data points and four independent parameters, $R^2 = 1.0$ since the terms of the equation can be uniquely determined. R_a^2 is a measure of how much information is contained in the model normalized by the number of parameters used to predict the dependent quantity. When the size of the data base is small, as was the case in this study, R_a^2 should be used to choose between models. Using R_a^2 ensures that the simplest, good predictive model is the one that is chosen.

Finding the best regression model begins by determining all the independent variables that might be good predictors of the dependent variable. When there are a large number of parameters, as is the case in this application, manually exploring each possible combination of variables would become a daunting task. Fortunately, statistical analysis software programs perform much of this work automatically. The SAS program was used for all the analyses in this project.^[28] The SAS programs used to choose models are included in appendix B of this report.

A stepwise linear regression procedure was used to find the best HIC and TTI models. This process proceeds by examining how good each individual parameter is at predicting the value of the dependent quantity. The best predictor was defined as the parameter that yielded the highest coefficient of regression (R^2). When the best single predictor was identified, the remaining parameters were reexamined to see which one, in combination

with the best predictor, would improve the R^2 the most. The process continued until the highest R^2 was obtained. This method is very useful since it systematically identifies the parameters that are the best predictors and eliminates parameters that are not good predictors of the dependent variable. Because the addition of any variable to the regression will result in a larger R^2 , other parameters must be examined to determine the best number of variables. The model with the largest adjusted R^2 is usually used because it is usually the simplest model that sufficiently explains the dependent variable. Judgement should also be used in choosing the optimum number of variables. Some variables may not be very reliable or may add little to the model. In such cases these variables may be eliminated. Engineering judgement may dictate that other variables should be in the model.

Once the best model of each form – i.e., linear or log-linear – was found, the different forms were compared. Since the dependent variable is different for the linear model than for the log-linear form the R^2 s cannot be compared directly to determine the best model. In order to compare models with different dependent variables, the dependent variable must first be geometrically standardized. The regressions are run again using the standardized dependent variables, and the model with the lowest mean square error is selected as the best model.

After determining the most appropriate model, the residuals of the regression should be checked for heteroscedasticity – nonrandomness. There should be no pattern in the residuals in order to meet the assumptions of ordinary least squares regression. After the errors are found to be randomly distributed, the model should be examined using professional judgement. The variables should seem like reasonable explanatory variables, and the coefficients should be of the appropriate magnitude and sign. Finally, the model should explain a satisfactory amount of the variance of the dependent variable before it is used as a predictor.

There are three primary injury mechanisms in side impact collisions: thoracic trauma, head injury and pelvic fracture. The HIC and the TTI were collected in 15 tests performed at the FOIL since 1983. The data from these tests are summarized in table 6. Stepwise regression analyses were performed to determine if there were relationships between any of the observed vehicle-based parameters and the values of TTI and HIC. Pelvic acceleration was not modeled since there has been no data collected as yet. The same type of modeling activity could be performed to estimate the accelerations of the pelvis based on vehicle-based parameters once sufficient data has been collected. The following sections summarize the findings of these investigations.^[29]

Occupant Risk Model

The occupant risk criteria recommended in *NCHRP Report 230* have evolved into the most important single evaluation criteria in testing roadside hardware.^[3] The ultimate objective of all safety hardware is to prevent or minimize the potential for injury to occupants of

vehicles that leave the traveled way. Unfortunately, establishing a linkage between parameters measured in crash tests and real occupants of vehicles in accidents has been an extraordinarily difficult task.

Report 230 introduced the concept of the flail space occupant risk criteria. The flail space method calculates the hypothetical impact velocity of an occupant with the interior of the vehicle. The flail space method described in *Report 230* is not adequate for side impacts since there is invariably significant intrusion into the passenger compartment. A method that accounts for this intrusion was discussed earlier in this report. The modified method was used to calculate the actual impact velocity of the anthropometric dummy with the interior of the vehicle. This was done so that comparisons could be made between the occupant risk and dummy-based measures of risk like TTI and HIC.

Relating the forces experienced by anthropometric test devices to the potential for serious injury is a challenging area of research that has been pursued by NHTSA, the military and the automotive design communities for decades. The measures of injury promoted by NHTSA are recommended since that agency has the most expertise and ability in the area of biomechanics and human tolerance. Conforming to the NHTSA recommendations will allow the roadside safety community to take advantage of a wealth of biomechanics experience while also facilitating the exchange of information between these two agencies in the future. While the HIC and TTI could certainly be improved, they have a better linkage to real human trauma than the flail space for side impacts.

Thoracic Trauma Model

A multiple linear regression analysis was performed on 15 tests of small cars side impacting a variety of poles. Each single parameter was investigated to see if any were good predictors of TTI by themselves. The best single-parameter predictor was the longitudinal distance between the dummy and the impact point (r). Even this parameter only had an R^2 of -0.52. The minus sign indicates that the TTI decreased with increasing values of r , the maximum TTI occurring at $r = 0$.

Since none of the parameters were good predictors of TTI alone, a multiple regression approach was examined. Simple linear models like equation 8 did not yield models with adequate R^2 . Log-linear models of the form of equations 9 through 11 were examined next. The first type of model explored used a variation of the exponential form.

$$TTI_j = \beta_0 \left\{ \frac{V_i^2}{c_e} \right\} \sum_{i=1}^n \beta_i^{X_{i,j}} \quad (12)$$

This form was chosen because the leading term, V_i^2/c_e , resulted in units of acceleration, the correct units for TTI. Physically, this term is one half of the average acceleration of the door surface assuming the vehicle comes to a complete stop. Other combinations of

parameters that yield acceleration were also examined. The average door acceleration, $\left(\frac{\dot{c}_i^2}{c_i}\right)$, was expected to be a good predictor of TTI since it involves both crush and crush rate. Since the TTI is the average acceleration of a body in contact with the door, this combination seemed like a good choice. However, the R^2 values for models with this combined parameter were not as good as the $\left\{\frac{V_i^2}{c_i}\right\}$ parameter. Another interesting combination involved the intrusion rate and the impact velocity. The term $\left(\frac{(V_i - \dot{c}_i)^2}{c_i}\right)$ was thought to be related to the occupant impact velocity. This term did not perform as well as the initial choice either so the impact velocity lead term was selected.

Having chosen the leading term for its physical significance and efficacy, the other parameters listed in table 6 were included as possible X_{ij} . The SAS program will interactively evaluate all possible combinations of the parameters and rank them based either on the best R^2 , the best adjusted R^2 or lowest Mallows' c_p statistic. Limiting the number of terms was a priority so the adjusted R^2 was used to initially rank the models. The adjusted R^2 takes into account the number of independent parameters. When this analysis was performed, the best model was found to be:

$$TTI = 0.35 \left\{ \frac{V_i^2}{c_e} \right\} 0.9957r^2 1.0904c_e \quad (13)$$

$$R^2 = 0.82$$

The model contains several interesting features in addition to the pseudo-acceleration term. The two most important predictors of TTI were the longitudinal position (r) and the amount of external crush (c_e). The model confirmed an observation that had been made during the testing: the position of the occupant at the time of impact is very important. When the impact is centered on the occupant, the dummy response will be much larger than when the dummy is located farther away from the impact point. A function that maximizes the TTI when the impact is centered on the occupant and decreases as the distance between the impact and occupant increased seemed reasonable. Because controlling the position of the dummy was nearly impossible, this model suggested that terms to account for dummy position must be included in all the models so that TTI values could be normalized to a similar scale. The values of TTI in two different tests may suggest completely erroneous conclusions if the effect of position is not addressed. A high TTI could result either from close proximity to the impact point or because of a particularly severe collision. It is desirable to eliminate the former and retain the latter effects in comparing one test to another.

The other exponential term was the external crush. Crush should be involved to some degree in predicting the risk of injury to the thorax because (1) it measures the energy dissipated by deforming the vehicle and (2) it reduces the flail space available to the impact-side occupant. Equation 13 shows that the relationship between crush and TTI is not a simple one. Crush appears in both the exponential term and in the denominator of the leading term. Figure 20 graphically shows the relationship between crush and TTI for an impact velocity of 40 mi/h (14 km/h) and longitudinal position of 10 in (250 mm).

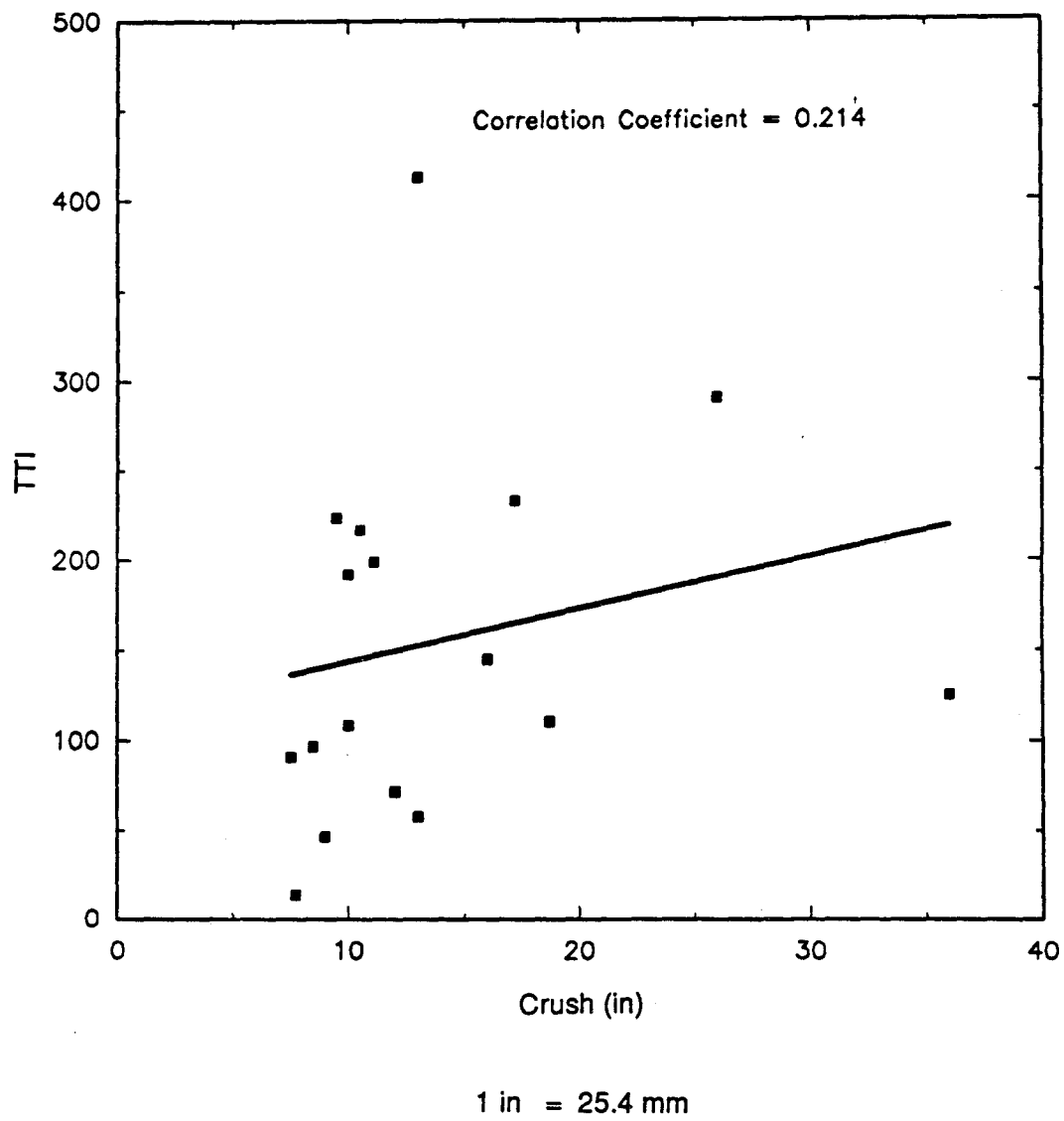


Figure 20. TTI versus the maximum external static crush.

Building this model illustrated the importance of accounting for dummy position. Although the lateral position was not found to be as important in this model, exponential terms to account for the longitudinal and lateral position of the dummy were included in all subsequent models.

The parameter form shown in equation 11 was also investigated. A similar stepwise regression procedure was followed to find the parameters that were most effective in predicting the TTI. The position terms were left in an exponential form since that aspect of the model seemed reasonable. The model with the fewest parameters and an R^2 above 0.85 was found to be:

$$TTI = 0.005 \{0.9173^r 0.9358^s\} V_i^{2.18} c_e^{0.96} \quad (14)$$

$$R^2 = 0.88$$

Like the previous model, crush and position were the two strongest predictors of TTI. The exponents of velocity and crush result in unusual units for the expression. The coefficient 0.005 must therefore have units to produce a value with units of g's. For this reason, these models are valid only for parameters with the proper units.

In a test with no dummy, three of these parameters (r , s , and V_i) are specified. Only crush is a measurable result of the test. The desirable, in-position location of an occupant is at $r = 10$ in (250 mm), $s = 6.5$ in (165 mm) and the standard impact speed is 44 ft/s (14 m/s)^[30]. The maximum allowable TTI recommended by NHTSA in FMVSS 214 is 90 g's^[5]. These values can be substituted into equation 16 and solved for the allowable crush. Doing so results in a criterion for the crush needed to minimize thoracic trauma.

$$c_e \leq 19 \text{ in (480 mm)} \quad (15)$$

If a vehicle sustained 10 in (483 mm) of crush, the expected TTI would be acceptable at a velocity of 44 ft/s (14 m/s). Equation 14 could also be used to estimate the probability of sustaining an $AIS > 3$ thoracic injury in a similar real-world collision. Table 7 shows the age-adjusted probability of sustaining an AIS great than 3 injury given a particular TTI.^[31] The distribution of TTI has been shown to be a Weibull extreme value distribution.^[9] The probability of sustaining an $AIS > 3$ injury based on the amount of crush observed could be estimated using table 7. The TTI is used to map the amount of crush to the appropriate level of risk. A crush of 24 in (605 mm) would imply a risk of severe thoracic injury of 0.31 to a correctly positioned occupant of a vehicle striking a pole at 30 mi/h (50 km/h).

While it seems reasonable that crush should be involved in predicting TTI, it should also be a function of the rate of crush. If the crush occurs slowly it should not pose much risk to the occupant whereas even a small amount of crush could be very dangerous if it occurs quickly in the vicinity of the occupant. Allowing another term in the predictive equation resulted in a model that includes both crush and crush rate.

Table 7. Probability of $AIS > 3$ thoracic injury.

TTI	Probability of $AIS > 3$ ^[31]	Allowable Crush Equation 14 in (mm)	Allowable T_{si} Equation 16
g's			
80	0.10	17 (434)	0.88
85	0.13	18 (462)	0.93
90	0.16	19 (490)	0.99
95	0.19	20 (519)	1.04
100	0.22	22 (547)	1.10
105	0.27	23 (576)	1.15
110	0.31	24 (605)	1.21
115	0.37	25 (633)	1.26
120	0.42	26 (662)	1.32

1 in = 25.40 mm

1 ft = 0.3048 m

1 ft/s = 0.3048 m/s

$$TTI = \frac{1}{33.33} \{0.9021^{0.9387^s}\} V_i^{2.5} \left\{ \frac{c_e^{1.25}}{10 \sqrt{c_i}} \right\} \quad (16)$$

$$R^2 = 0.90$$

The components of this model seem reasonable: severity should increase as the occupant gets closer to the impact point (r and s) and severity should be a function of the impact velocity (V_i) since this is a measure of the total amount of kinetic energy at the start of the impact event. Passenger compartment crush and crush rate were also thought to be directly related to the TTI since thoracic injuries are caused by contact with the side door panels.

In a test with no dummy, three of these parameters (r , s , and V_i) are specified. Only crush and crush rate are measurable results of the test. The desirable, in-position location of an occupant is at $r = 10$ in (250 mm), $s = 6.5$ in (165 mm) and the standard impact speed is 44 ft/s (14 m/s).^[30] The maximum allowable TTI recommended by NHTSA in FMVSS 214 is 90 g's.^[5] These values can be substituted into equation 16 and solved for the quantity $T_{si} = \left(\frac{c_e^{1.25}}{4 \sqrt{c_i}} \right)$. T_{si} is a vehicle-based parameter that could be used to link the crash test performance to the risk of severe injury in a similar real-world accident. Doing so results in a criterion for the crush and crush rate needed to minimize thoracic trauma.

$$1 \geq \left(\frac{c_e^{1.25}}{10 \sqrt{c_i}} \right) = T_{si} \quad (17)$$

If the crush and crush rate result in a value of equation 17 less than 1, the probability

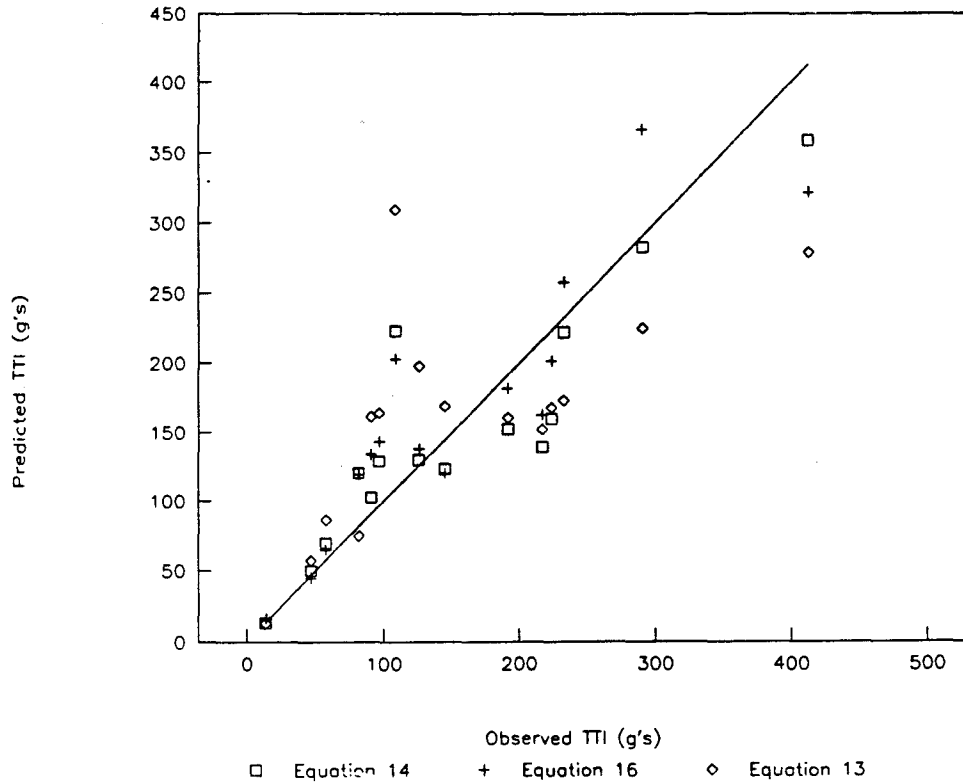


Figure 21. Observed versus predicted TTI.

of observing a TTI greater than 90 is relatively small. This model provides the highest R^2 and involves only two observable measures of test performance: c_e and \dot{c}_i . As with equations 14 and 16, the value of TTI can be used to map T_{si} to the probability of experiencing an $AIS > 3$ injury. Observing a value of T_{si} greater than 1.0 in a crash test would suggest an unacceptably high risk of severe thoracic injury to correctly positioned occupants.

While all the models described above yielded good results in terms of the R^2 , there are potential difficulties that should be recognized. The data is limited to a very narrow range of test conditions and test devices. These expressions for predicting TTI were developed using the results of the 15 side impact tests of slip-base poles and ESV poles summarized in table 6. The degree to which these models will predict TTI scores for other types of devices is not known. No other types of devices were included in the test data. The models are probably good representations of the performance of poles, but it remains to be proven that they are valid in test with other types of hardware like terminals, small signs or narrow crash cushions.

Figure 21 shows the relationship between the observed values of TTI and those predicted by equations 13, 14 and 16. The predictions are generally quite good. The scatter appears to be fairly random but there are traces of a possible nonlinear functional relationship between the observations and predictions. This nonheteroscedacity suggests

there may be effects that are not adequately accounted for in the models. These effects may be related to unmeasured parameters.

The test conditions available were also limited to velocities between 20 mi/h (32 km/h) and 40 mi/h (64 km/h). The fidelity of the models outside this range should be questioned since there is no data beyond the tested conditions. The range of crush values in these tests was between 6 and 35 in (200 to 900 mm). Observed crush rates were as high as 33 ft/s (10 m/s). These expressions might not yield appropriate estimates for tests where the crush or crush rate are outside the tested range.

A more fundamental concern is the ability of these macroparameters to predict dummy responses that are precipitated by very small events that occur during the collision. The TTI, since it is an acceleration, should be very sensitive to the stiffness of the object the torso strikes. The TTI could be quite different if the thorax contacts the arm rest or the flat surface of the door. The response will be different if the shoulder strikes the lower window frame or if the pelvis strikes the middle of the inner door. These events are impossible to control and nearly as difficult to observe. The only parameters that can be observed and measured with any confidence are large-scale responses like the vehicle crush, crush rate, change in velocity, and vehicle accelerations. Since these parameters represent only part of the injury mechanism, it should not be surprising that there is and will always be an appreciable amount of random error involved in the measurements. These expressions should be used as a guide when direct measures of the TTI are not available. More experience with using these models will help establish if they are useful and reasonable measures of hypothetical severity.

Head Injury Criteria

The same type of regression analysis was performed to find models for the HIC. The results of this analysis were not as attractive as the TTI model described in the previous section because of lower R^2 . It is presented here to serve as an approximate guide for tests where no dummies are included.

Unfortunately, the HIC was not developed to measure head injury potential in side impacts. The differences between longitudinal and lateral head impact tolerance and the degree to which the Part 572 head form predicts human injury have been debated but no consensus has been reached.^[13] The head is probably *less* tolerant in lateral impacts than in frontal impacts so the HIC should certainly be no greater than 1000. There is a great need for the biomechanics research community to address the issue of an appropriate lateral HIC limit or, more generally, head injury criteria for the side of the head. A $HIC = 1000$ has been used in a recent study of head form impacts with upper vehicle-interior structures like the A-pillar, roof rails and B-pillar.^[32] A limit of 1000 appears to be the best available link between the dynamics of an impacting head and the potential for serious injury.

Most of the 15 tests were conducted with the dummy head aligned with the impacting pole ($r = 0$). This caused exceptionally high HIC values since there was often direct contact between the pole and the head. This extreme test condition may be more demanding than the side impact dummy capabilities. For this reason, a longitudinal impact point (r) of 10 in (250 mm) was recommended for future tests.^[30] The severity of the loading caused problems in developing a model for HIC. The $r = 0$ position appears to represent a singularity in the response of the dummy.

The first HIC model developed was similar to the first TTI model. The lead term is the same although it's units are not particularly significant since HIC has nonstandard units. Other leading terms were attempted but $\left(\frac{V_i^2}{C_e}\right)$ consistently provided the models with the best R^2 . Terms for position (r and s) were included to account for the wide variety of actual pre-impact dummy positions. The parameter r was the best single predictor of HIC. The best four parameter model using the exponential log-linear form as found to be:

$$HIC = 9.60 \left\{ \frac{V_i^2}{C_e} \right\} 0.9928^{r^2} 0.7564^s 0.9991^{V_i^2} 1.0031^{C_{area}} \quad (18)$$

$$R^2 = 0.42$$

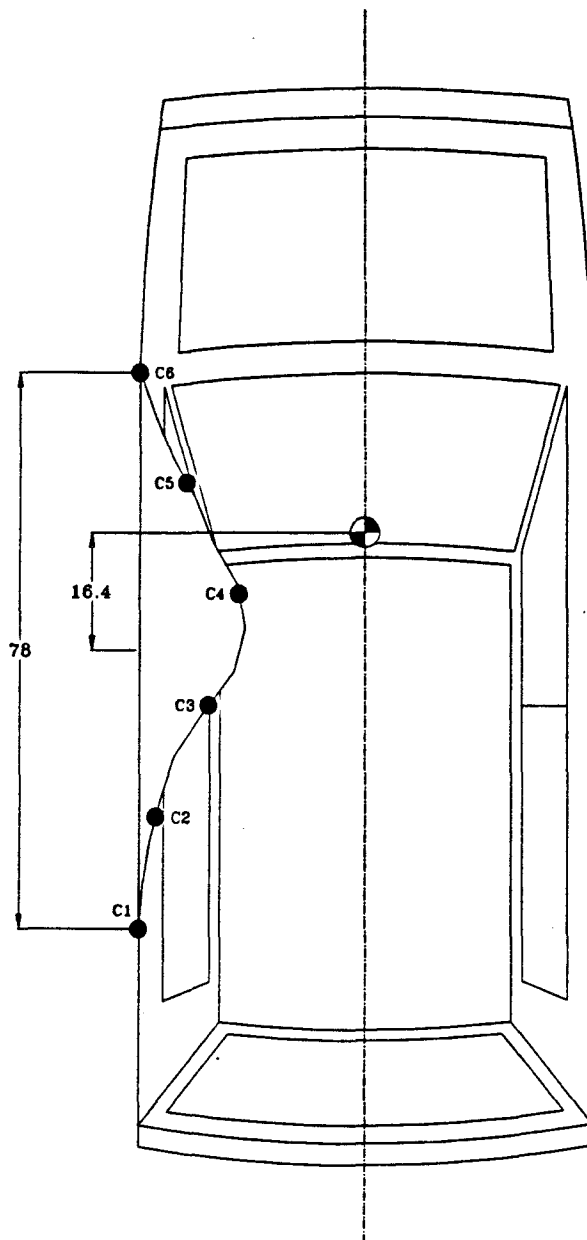
The R^2 for this model was low. The predictive terms, V_i and C_{area} were also disappointing since they are both measures of energy: preimpact energy in the case of V_i and the energy of deformation in the case of C_{area} . Neither V_i or C_{area} is thought to be very close to the actual mechanism that causes injury in side impacts. Figure 22 shows an example of a 6-point NHTSA sketch from which the damaged area can be calculated. C_{area} was calculated by averaging the six crush measurements at the moulding-line (where the moulding strip is attached on the side of a passenger car) and multiplying by the length of the damage.

Using the parameter form of the log-linear mixed parameter model results in a similar expression involving the dummy positions and the area crushed.

$$HIC = 31.51 \{0.8251^r 0.7400^s\} C_{area}^{1.02} \quad (19)$$

$$R^2 = 0.54$$

While this model was an improvement over the last in terms of a higher R^2 , the parameter C_{area} is not a particularly helpful measure of hardware effectiveness. This term is presumably a surrogate measure of the amount of energy that was dissipated through vehicle deformation. One definition of risk is exposure to energy; whenever an occupant is in an environment where there is more energy there will be a higher risk of injury.^[33] It is interesting that the HIC seems to be related to the energy dissipated by vehicle deformation rather than the total amount of kinetic energy available in the collision ($\frac{1}{2}mV_i^2$).



91S046

1984 Honda Civic

30 mi/h

MELT S.I.

AUGUST 27, 1991

NHTSA CRUSH POINTS

LOCATION	CRUSH (in)
C1	0
C2	2.4
C3	9.9
C4	14.2
C5	6.7
C6	0

LENGTH OF CRUSH: 78 in

DISTANCE FROM MIDPOINT OF

CRUSH TO C.G. OF CAR: 16.4 in

MAXIMUM CRUSH: 15 in

$$C_{area} = \left(\frac{0.0+2.4+9.9+14.2+6.7+0.0}{6} \right) \times 78 = 432 \text{ in}^2$$

$$1 \text{ in} = 25.4 \text{ mm}$$

$$1 \text{ in}^2 = 15.55 \text{ mm}^2$$

$$1 \text{ mi/h} = 1.61 \text{ km/h}$$

Figure 22. Six-point damage sketch for calculating C_{area} .

Table 8. Probability of $AIS > 3$ head injury.

HIC	Probability of $AIS > 3$ ^[12]	Allowable C_{area} Equation 19 in[2]	Allowable H_{si} Equation 21
400	0.03	542	0.40
600	0.05	807	0.59
800	0.10	1069	0.79
1000	0.18	1331	0.99
1200	0.31	1591	1.19
1400	0.47	1851	1.38
1600	0.64	2110	1.58
1800	0.79	2368	1.78

$$1 \text{ in}^2 = 645 \text{ mm}^2$$

This expression could be used to solve for a crush area deformation criteria by setting $HIC = 1000$ and assuming the dummy is correctly positioned. Doing so would suggest that as long as the damaged area observed is less than 1300 in^2 (0.84 m^2) the HIC for a correctly positioned hypothetical occupant would be unlikely to sustain a serious head injury.

$$C_{area} \geq 1300 \quad (20)$$

The HIC, like the TTI, has been related to the probability of sustaining an $AIS > 3$ injury.^{[12],[32]} The HIC could be used as a link between the observed area of crush and the probability of injury, $P(AIS > 3)$. Table 8 shows the relationship between the HIC and $P(AIS > 3)$ as well as several links to observable crash test parameters. It is important to recognize that the information in table 8 was developed for a hypothetical occupant who is correctly positioned at the time of impact ($r = 10 \text{ in}$ (250 mm), $s = 6.5 \text{ in}$ (165 mm)). An occupant who is closer to the impact point at the time of collision, would be at much higher risk since, as shown by equation 19, the HIC appears to decay exponentially as the distance from the impact point increases.

While it can be argued that crush and crush rate are also measures of the energy dissipated through vehicle deformation, these quantities should be more closely related to the HIC since they measure the amount and the speed of intrusion into the passenger compartment. The best five parameter model included crush, crush rate, and the actual occupant impact velocity.

$$HIC = 49(10)^3 \{0.8251^r 0.7400^s\} \left(\frac{5 c_e^{1.64}}{\dot{c}_i^{1.1} V_o^{0.14}} \right) \quad (21)$$

$$HIC = 49(10)^3 \{0.8251^r 0.7400^s\} H_{si} \quad (22)$$

$$R^2 = 0.55$$

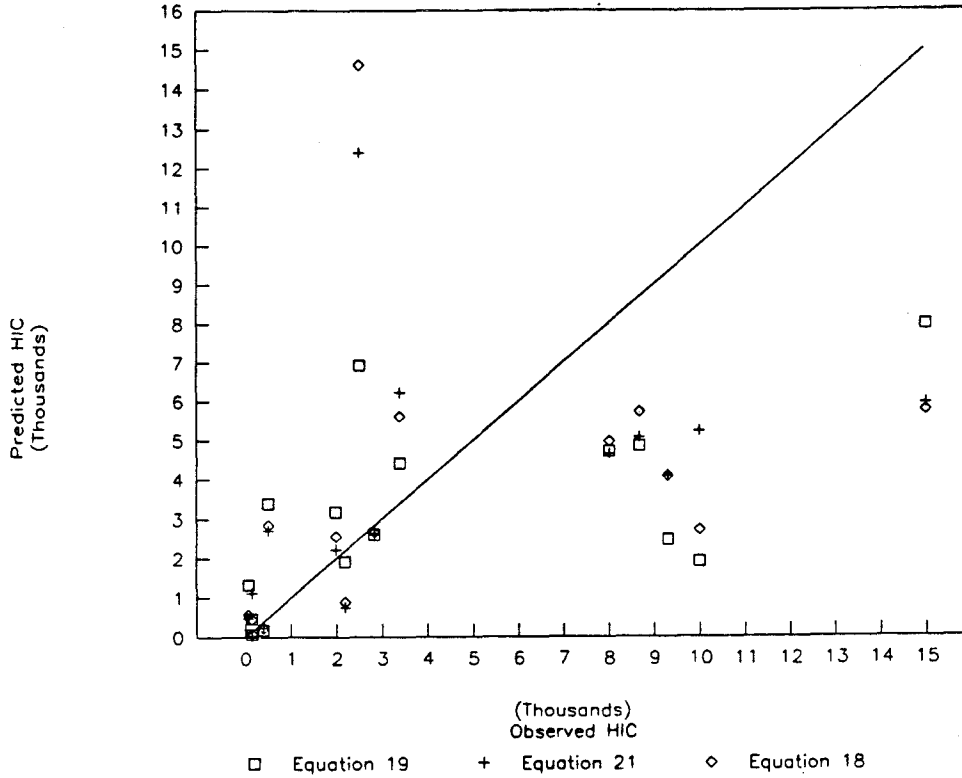


Figure 23. Observed versus predicted HIC.

When there is no dummy in the test vehicle, the above expression can be solved for limiting values of the quantity $H_{si} = \left(\frac{5 c_e^{1.64}}{c_i^{1.1} V_o^{0.14}} \right)$. H_{si} is a side impact head injury scale that uses vehicle-based kinematics to predict the probability of an $AIS > 3$ head injury. Substituting $HIC = 1000$, $r = 10$ in (250 mm), and $s = 6.5$ in (165 mm), yields a value of 1.0. An approximate criteria that would predict acceptable HIC values could be stated as:

$$1 \geq \left(\frac{5 c_e^{1.64}}{c_i^{1.1} V_o^{0.14}} \right) = H_{si} \quad (23)$$

This criteria suggests that HIC is related to the combined effects of crush, crush rate, and occupant impact velocity. The HIC can be used to link the parameter H_{si} to the probability of sustaining an $AIS > 3$ injury. Table 8 shows the relationships between H_{si} and the probability of $AIS > 3$ injury.

Figure 23 compares the observed HIC models to the predictions of equations 18, 19 and 21. There is a large amount of experimental scatter in figure 23 that graphically represents the relatively low R^2 s for these HIC models. The two extreme HIC values in table 6 were excluded from this graph to improve the clarity of the remaining data. The models seem to be relatively good predictors when the HIC is below the threshold value of 1000. The models did not provide good estimates for extreme values (those above 1000).

As with the TTI models described in the last section, these models may not be appropriate for devices that are not breakaway poles and for impacts outside the range of typical values used in building the regression models. These equations are presented as a guide for tests where it is not possible to use a dummy in the test vehicle. These models, due to the underlying data, should only be used in tests where there is a possibility of direct contact between the head and the intruding object. In tests of guardrail terminals, for example, contact between the head and the terminal is unlikely so the HIC should not be evaluated. The HIC should always be evaluated for tall, narrow objects like luminaires, utility poles and signs.

Model Refinements

The models presented in this report should be viewed as first order approximations that will invariably change as more experimental data is obtained. While the particular details of the models for TTI and HIC may change as new data is incorporated, the approach described for building probabilistic models described above should remain unchanged. This probabilistic approach can be used to link test performance to the expected performance of these devices in real-world accidents. The equations presented in the previous sections are the best available predictive models given the data available. Improvements in the models should be pursued to try and better understand the injury mechanisms at work in side impact fixed-object collisions.

Obtaining additional crash test data is the best way to improve these models. In the course of this testing a great deal has been learned about side impact collisions and improvements in the type of data that can be acquired have been made. For example, the tests that served as the basis for the severity models estimated the intrusion rate using the on-board film. For the seven tests that were derived from the literature, film analysis was the only available technique that could be used. Later tests performed in this project included a string-pot potentiometer to measure the intrusion rate directly. Film analysis introduces errors due to imprecise pointing, poor film resolution in on-board shots, and blocked views that occur during the impact event. The estimates of intrusion rate were very different in the tests that used the transducer than in tests where film analysis was used. While some of the differences are doubtless due to differences in severity, it seems plausible that the film analysis technique underestimates the intrusion rate. Test conditions have also played a role in obscuring some of the dummy responses. Dummy position was found to be very important but difficult to control. Any new testing should attempt to improve the control over the dummy's initial position at impact. As mentioned above in describing the HIC modelling effort, impact location has made modelling the HIC in particular very difficult. There appears to be a singularity in the HIC response when the longitudinal position of the dummy head is aligned with the impacting object. New tests should ensure that the head does not directly contact the test device. Tests that take advantage of these recommendations should result in higher quality data that can in turn be used to build higher quality severity models.

Table 9. Data elements required in side impact crash tests.

Parameter	Symbol	Acquisition Device
Impact Velocity	V_i	Film
Actual Dummy Impact Velocity	V_{occ}	Calculations
Maximum static vehicle crush (exterior)	c_e	NHTSA 6-point sketch
Area of crush (exterior)	C_{area}	NHTSA 6-point sketch
Maximum dynamic intrusion (interior)	c_i	Displacement Transducer
Average intrusion rate (interior)	\dot{c}_i	Displacement Transducer
Maximum 10-ms vehicle acceleration prior to dummy contact with interior.	a_{pc}	Vehicle accelerometers
Maximum 10-ms vehicle acceleration during dummy contact with interior.	a_{dc}	Vehicle accelerometers
Maximum 10-ms vehicle acceleration after dummy contact with interior.	a_{rd}	Vehicle accelerometers
Thoracic Trauma Index	TTI	Anthropometric Dummy
Head Injury Criteria	HIC	Anthropometric Dummy
Maximum pelvis acceleration	a_p	Anthropometric Dummy
Longitudinal distance from the center of the dummy head to impact point	r	Onboard Film
Lateral distance from the left side of the dummy head to edge of passenger compartment	s	Onboard Film
Distance from impact point to front axle	D	Post Test Measurement

Recommendations for performing side impact crash test of roadside structures were developed in this project. These recommendations are contained in the third volume of this report.^[30] New tests should be performed according to these recommendations to minimize variations between tests. Table 9 shows a list of test parameters that should be observed and recorded in each side impact test. Some of these data elements were not used in the foregoing analysis but have been included because they may provide a useful insight in future tests. For example, the 10 ms average acceleration during the three phase of dummy motion (pre-contact, contact, and post contact) are suggested because these values may be better predictors than those listed in table 6.

The recommended test and evaluation criteria suggest a single 30 mi/h (50 km/h) full-broadside test that includes a fully instrumented anthropometric dummy. The tests evaluated in this project have demonstrated several effects that should not be reinvestigated. The effect of longitudinal position, for example, was shown to be very important in predicting the TTI and HIC. New tests should use the recommended seating position and impact point to minimize the effect of impact point. Likewise, the impact velocity was shown to be important because it measures the amount of pre-impact kinetic energy. New tests should focus on the single recommended impact velocity of 30 mi/h

(50 km/h). The purpose of future test series should be to determine the relationship between measurable test quantities like crush, crush rate and deceleration.

Future tests should include other types of roadside structures and there should be at least three identical tests of each device so that the experimental scatter can be evaluated. This will also help develop a better understanding of the effect of dummy initial position in similar tests. The values of all the data elements shown in table 9 should be collected and entered into a data base like that shown in table 6.

The process of reanalyzing the data to build refined models should be very straightforward. The new experimental observations should be added to the data in the SAS programs shown in appendix B and re-run. The step-wise regression procedure (the `maxr` option to the `model` statement) should be used. This procedure incrementally adds parameters that improve the R^2 . Using the `selection=adjrsq` option is also useful for evaluating the R^2_{adj} for these models. The model yielding the best R^2 with as few parameters as possible should be selected as the best model. Once the parameters involved in a good model have been developed, the SAS program can be rerun with the `P` option to find specific information about the model. The values of the exponents and coefficients would change to reflect the addition of new data.

Chapter 5. Summary

This report contains a detailed summary of the 1991 side impact crash testing program conducted at the Federal Outdoor Impact Laboratory. The results of previous side impact crash tests are also presented along with descriptions of the associated test procedures. The devices tested included energy absorbing, slipbase and transformer base poles, and four guardrail terminal designs. In addition, several modifications of the occupant risk criteria recommended in *Report 230* and other injury measures related to the thoracic and head regions of the body are presented.

Finally, regression models that link the crash test performance to the probability of occupant injury in the field were developed. These models predicted the TTI and the HIC based on vehicle-based observable parameters that could be measured in a crash tests. The predicted TTI and HIC could then be used to estimate the probability of injury using injury distributions developed in human tolerance research. These vehicle-based criteria, while preliminary, demonstrate a method that could be used to hypothesize about the survivability of similar real-world collisions.

Side impact collisions with fixed objects along the roadside are an important accident scenario that has been often overlooked in developing roadside hardware. The tests performed in the project helped to demonstrate the importance and severity of this type of collision.

A. Side Impact Crash Tests of Roadside Objects

The following is a list of side impact appurtenance crash tests. The list contains a test number, date, and a brief description of the test. The authors have, to the best of their ability, attempted to make this list a comprehensive list of side impact crash tests involving safety hardware throughout the world. Abbreviations used in this appendix are shown below:

FOIL Federal Outdoor Impact Laboratory, Turner-Fairbank Highway Research Center, 6300 Georgetown Pike, McLean, Virginia 22101, USA.
TRC Transportation Research Center of Ohio, State Route 33, Logan County, East Liberty, Ohio 43319, USA.
TRRL Transportation Road Research Laboratory, Crowthorne, Berkshire, U.K.
TTI Texas Transportation Institute, College Station, TX, USA.
VTI Väg-och Trafik Institutet, S-581 01 Linköping, Sweden

Test Number	Date	Description
SW1	67	Conducted by TRRL at TRRL, Crowthorne, UK: Slip-base luminaire support (4 bolt base) 69 mi/h (111 km/h) impact speed, impact angle 45 degree. Non-tracking yawing impact. Impact point behind the rear wheel well, right-rear quarter panel. 1962 2,400 lb (10.7 kN) 4-door passenger car. NOTE: No dummy used in this test.
3114-C6	1/77	Conducted by TTI at TTI: Slip-base luminaire support (Union Metal, circular — 3 bolt base) 20 mi/h (32.2 km/h)-broadside (sliding), 71 Chevrolet Vega [2,670 lb (11.9 kN)]. NOTE: No dummy used in this test.
FHWA Contract DTFH61-C-81-00036, <i>Laboratory Procedures to Determine the Breakaway Behavior of Luminaire Supports in Mini-sized Vehicle collisions:</i>		
1469-4A82	4/82	Slip-base surrogate pole, 30 mi/h (48.3 km/h)-broadside into dummy (sliding), 76 Volkswagen Rabbit (1,850 lb (8.2 kN) plus weight of SID dummy).

Test Number	Date	Description
1469-5A82	6/82	Slip-base surrogate pole, 30 mi/h (48.3 km/h)- at an angle of 60 degrees into A pillar (sliding), 76 Volkswagen Rabbit
1469-SI-1-85	6/85	<u>Conducted at FOIL:</u> Rigid pole, 25 mi/h (40.3 km/h)-broadside at dummy position, 79 Honda Civic. NOTE: No dummy used in this test.
1469-SI-2-85	7/85	<u>Conducted at FOIL:</u> Rigid pole, 25 mi/h (40.3 km/h)-broadside at dummy position, 79 Volkswagen Rabbit. NOTE: No dummy used in this test.
1469-SI-3-85	7/85	<u>Conducted at FOIL:</u> Rigid pole, 25 mi/h (40.3 km/h)-broadside at dummy position, 79 Dodge Colt. NOTE: No dummy used in this test.
1469-SI-4-85	7/85	<u>Conducted at FOIL:</u> Slip-base luminaire sup- port, 30 mi/h (48.3 km/h)-broadside into dummy, 79 Honda Civic.
1469-SI-5-85	7/85	<u>Conducted at FOIL:</u> Slip-base luminaire sup- port, 30 mi/h (48.3 km/h)-broadside into dummy, 79 Volkswagen Rabbit.
1469-SI-6-85	8/85	<u>Conducted at FOIL:</u> Slip-base luminaire sup- port, 30 mi/h (48.3 km/h)-broadside into dummy, 79 Dodge Colt.
1469-SI-7-85	10/85	<u>Conducted at FOIL:</u> Slip-base luminaire sup- port, 30 mi/h (48.3 km/h)-broadside into dummy, 79 Dodge St. Regis.
1469-SI-8-85	12/85	<u>Conducted at FOIL:</u> Rigid pole, 10 mi/h (16.1 km/h)-broadside at dummy position (no dummy used), 79 Dodge St. Regis.

Test Number	Date	Description
840629	6/84	<p><u>Conducted in Ohio:</u> Rigid pole, 20 mi/h (32.2 km/h) – at an angle of 45 degrees into A pillar, approximately (impact point 34.5 in (876 mm) forward of wheelbase midpoint – vehicle crabbed & rolling at impact), 81 Volkswagen Rabbit (2,065 lb (9.2 kN) plus 2 SID dummies and 185 lb (822.9 N) of surrogate fuel = 2,593 lb (11.5 kN) total). NOTE: One SID dummy placed in driver position and in left rear passenger position, respectively.</p>
840706	7/84	<p><u>Conducted in Ohio:</u> Rigid pole, 20 mi/h (32.2 km/h) – at an angle of 45 degrees slightly rearward of the A pillar, approximately (impact point 26.5 in (673 mm) forward of wheelbase midpoint – vehicle crabbed & rolling at impact), 81 Volkswagen Rabbit (2,065 lb (9.2 kN) plus 2 SID dummies and 185 lb (822.9 N) of surrogate fuel = 2,593 lb (11.5 kN) total). NOTE: One SID dummy placed in driver position and in left rear passenger position, respectively.</p>
840803	8/84	<p><u>Conducted in Ohio:</u> Rigid pole, 20 mi/h (32.2 km/h) – at an angle of 45 degrees into the driver dummy shoulder, approximately (impact point 6.5 in (165 mm) forward of wheelbase midpoint – vehicle crabbed & rolling at impact, 81 Volkswagen Rabbit (2,020 lb (8.9 kN) plus 2 SID dummies, 1 child dummy + infant seat and 185 lb (822.9 N) of surrogate fuel = 2,494 lb (11.1 kN) total). NOTE: One SID dummy placed in driver position and in left rear passenger position, respectively. Child dummy and infant seat placed in right rear passenger seat.</p>

Test Number	Date	Description
840816	8/84	<p><u>Conducted in Ohio:</u> Rigid pole, 20 mi/h (32.2 km/h) – at an angle of 45 degrees into the driver dummy shoulder, approximately (impact point 9.0 in (229 mm) forward of wheelbase midpoint – vehicle crabbed & rolling at impact), structurally modified 77 Volkswagen Rabbit (1,990 lb (8.9 kN) plus 2 SID dummies and 262 lb (1.2 kN) of surrogate fuel + modifications = 2,600 lb (11.6 kN) total). NOTE: One SID dummy placed in driver position and in left rear passenger position, respectively.</p>
FHWA Contract DTFH61-86-Z-00047, <i>Full-scale Side Impact Testing</i>		
1785-SI-1-87 (87S095)	7/87	<p><u>Conducted at FOIL:</u> Slip-base luminaire support, 30 mi/h (48.3 km/h)-broadside into dummy, 80 Plymouth Champ.</p>
1785-SI-2-87 (87S096)	7/87	<p><u>Conducted at FOIL:</u> Transformer-base luminaire support, 30 mi/h (48.3 km/h)-broadside into dummy, 80 Dodge Colt. NOTE: Support did not breakaway.</p>
1785-SI-3-87 (87S105)	10/87	<p><u>Conducted at FOIL:</u> Slip-base luminaire support, 30 mi/h (48.3 km/h)-broadside into dummy, 81 Dodge Colt.</p>
1785-SI-4-87 (87S106)	10/87	<p><u>Conducted at FOIL:</u> Slip-base luminaire support, 30 mi/h (48.3 km/h)-broadside into dummy, 80 Plymouth Champ.</p>
1785-SI-5-87 (87S107)	10/87	<p><u>Conducted at FOIL:</u> Slip-base luminaire support, 30 mi/h (48.3 km/h)-broadside 12 in (305 mm) behind dummy, 81 Plymouth Champ.</p>
1785-SI-6-88 (88S006)	4/88	<p><u>Conducted at FOIL:</u> Slip-base luminaire support, 30 mi/h (48.3 km/h)-broadside 12 in (305 mm) forward of dummy, 80 Plymouth Champ. NOTE: Support did not breakaway.</p>

Test Number	Date	Description
1785-SI-6A-88 (88S007)	5/88	<u>Conducted at FOIL:</u> Slip-base luminaire support, 30 mi/h (48.3 km/h)- broadside 12 in (305 mm) forward of dummy, 80 Plymouth Champ. NOTE: Repeat of previous test – all transducer data lost.
1785-SI-7-88 (88S008)	5/88	<u>Conducted at FOIL:</u> Slip-base luminaire support, 30 mi/h (48.3 km/h)- broadside 24 in (610 mm) forward of dummy, 80 Dodge Colt.
1785-SI-8-88 (88S009)	6/88	<u>Conducted at FOIL:</u> Slip-base luminaire support, 30 mi/h (48.3 km/h)- broadside into dummy, 81 Plymouth Champ.

Tests performed at the Swedish Road and Traffic Research Institute (VTI) in Linköping, Sweden

890919-1	30 mi/h (48-km/h) collision between a Saab 9000 and an ESV pole.
890926-1	30 mi/h (48-km/h) collision between a 1,740-lb (790-kg) Honda Civic 1200 SBA and an ESV pole
891017-1	30 mi/h (48-km/h) collision between a 2,775-lb (1,260-kg) Saab 99 GL and a luminaire support.
891017-2	30 mi/h (48-km/h) collision between a 2,555-lb (1,160-kg) Saab 99HK and an ESV pole.
891108-1	30 mi/h (48-km/h) collision between a 2,600-lb (1,180-kg) Saab 99HK and an aluminum luminaire support.
891110-1	30 mi/h (48-km/h) collision between a 2,700-lb (1,210-kg) Saab 99HK and an ESV pole.
891114-1	20 mi/h (32-km/h) collision between a (1,850-lb) 840-kg Renault 5R and a luminaire support.
891115-1	64 mi/h (103-km/h) collision between a (1,850-lb) 840-kg Renault 5R and a luminaire support.

Test Number	Date	Description
FHWA Contract DTFH61-91-Z-00002, <i>Maintenance and Support of the Federal Outdoor Impact Laboratory:</i>		
90S058	12/90	<u>Conducted at FOIL:</u> Slip-base luminaire support, 30+ mi/h (48.3+ km/h)-broadside into dummy, 88 Ford Taurus (3,340 lb (14.9 kN) plus weight of SIS dummy). NOTE: Bolt clamping force reduced to 6.5 kips (28.9 kN) each (roughly 1/2 of prior tests).
90S059	12/90	<u>Conducted at FOIL:</u> Slip-base luminaire support, 30 mi/h (48.3 km/h)-broadside into dummy, 88 Honda Civic (2,032 lb (9.0 kN) plus weight of SIS dummy). NOTE: Bolt Clamping force reduced to 6.5 kips (28.9 kN) each (roughly 1/2 of prior tests).
FHWA Contract DTFH61-88-C-00092, <i>Side Impact Crash Testing.</i>		
91S001	1/10/91	<u>Conducted by FOIL:</u> ESV energy absorbing luminaire support, 30 mi/h (48.3 km/h), broadside, impact located on the dummy shoulder, Dodge Colt. FHWA Report No. FHWA-RD-91-088.
91S002	1/18/91	<u>Conducted by FOIL:</u> ESV energy absorbing luminaire support, 20 mi/h (32.2 km/h), broadside, impact located on the dummy shoulder, Dodge Colt. FHWA Report No. FHWA-RD-92-031.
91S003	1/25/91	<u>Conducted by FOIL:</u> ESV energy absorbing luminaire support, 30 mi/h (48.3 km/h), broadside, impact located on the dummy shoulder, Honda Civic. Base fractured. FHWA Report No. FHWA-RD-92-032.
91S004	2/11/91	<u>Conducted by FOIL:</u> 3-bolt slip-base luminaire, 20 mi/h (32.2 km/h), broadside, impact centered on occupant shoulder. Dodge Colt. FHWA Report No. FHWA-RD-92-033.

Test Number	Date	Description
91S005	2/14/91	<u>Conducted by FOIL:</u> ESV energy absorbing luminaire support, 40 mi/h (64.4 km/h), broadside, impact located on the dummy shoulder, Dodge Colt. FHWA Report No. FHWA-RD-92-034.
91S006	2/21/91	<u>Conducted by FOIL:</u> 3-bolt slip-base luminaire, 20 mi/h (32.2 km/h), broadside, impact centered on occupant shoulder. Dodge Colt. FHWA Report No. FHWA-RD-92-035.
91S007	2/28/91	<u>Conducted by FOIL:</u> 3-bolt slip-base luminaire, 40 mi/h (64.4 km/h), broadside, impact centered on occupant shoulder. Dodge Colt. FHWA Report No. FHWA-RD-92-036.
91S036	7/16/91	<u>Conducted by FOIL:</u> 30-mi/h (48.3-km/h) broadside collision centered on the middle of the door of a breakaway cable terminal (BCT) with a Honda Civic Si. FHWA Report No. FHWA-RD-92-046.
91S037	7/23/91	<u>Conducted by FOIL:</u> 30-mi/h (48.3-km/h) broadside collision centered on the middle of the door of an eccentric loader breakaway cable terminal (ELT) with a Honda Civic Si. FHWA Report No. FHWA-RD-92-047.
91S038	8/01/91	<u>Conducted by FOIL:</u> 30-mi/h (48.3-km/h) broadside collision centered on the middle of the door of a modified eccentric loader breakaway cable terminal (MELT) with a Honda Civic Si. FHWA Report No. FHWA-RD-92-051.
91S046	8/27/91	<u>Conducted by FOIL:</u> 30-mi/h (48.3-km/h) broadside collision centered on the middle of the door of a modified eccentric loader breakaway cable terminal enhanced for side impacts (MELT-SI) with a Honda Civic Si. FHWA Report No. FHWA-RD-92-052.

B. SAS Programs

The SAS programs used for the regression modelling analysis are included in this appendix. If new test data becomes available, the new data may be added to these programs to generate updated models that take advantage of the new data. These programs were written using the SAS/STAT statistical analysis software package. These programs were written using version 6.03 for Unix workstations.

```
*-----*
The following program finds a regression model
for the Thoracic Trauma Index (TTI).
written by: M.Ray
last change: 4-20-92
*-----*;
title 'Thoracic Trauma Index Model (Imperial Units)';
data dummy;
input
test $    tti  r vi vo  s c cdot a c_area;
cards;
91s001    145  0 44 15 12 16 23  4 252
91s002     47  0 26 26  0  9 13  2 170
91s003     97  0 44 12  3  9 12  2 191
91s004     82  0 28 26  0 19 17 12 350
91s005    109  0 61 14  7 10 24  7 258
91s007    413  0 58 18  2 13 27  6 271
87s096    291  0 42 33  5 26 16  8 780
87s105    224  0 45 10  2 10 10  2 263
87s106    192  0 44 13  2 10 11  2 242
87s107     58 12 44 17  2 13 14  3 250
88s006    126 12 41 14  5 36 19  5 942
88s008     14 24 42 12  3  8  4  4 228
88s009     91  0 43 18  4  8  8  2 211
1469s4    217  0 43 24  4 11 12  4 250
1469s6    233  0 44 19  4 17 16  1 385;
data lnDummy;
set dummy;
ltti=log(tti);
lc=LOG(c);
lcdot=LOG(cdot);
lvi=LOG(vi);
proc reg;
model ltti= r s lvi lc  lcdot/P;
run;
```

```

*-----*
The following program finds a regression model for the
Head Injury Criteria (HIC).
    written by: M.Ray        last change: 4-20-92
*-----*

options pagesize=40;
options linesize=80;
title 'Head Injury Criteria Model: Unbounded HIC (Imperial units)';
data dummy;
input
test $   hic   r vi vo   s c cdot a c_area;
cards;
91s001   398   0 44 15 12 1.333 23   4 252
91s002 44101   0 26 26   0 0.750 13   2 170
91s003   503   0 44 12   3 0.750 12   2 191
91s004  2513   0 28 26   0 1.583 17 12 350
91s005   139   0 61 14   7 0.833 24   7 258
91s007 17776   0 58 18   2 1.083 27   6 271
87s096  3385   0 42 33   5 2.167 16   8 780
87s105  8684   0 45 10   2 0.833 10   2 263
87s106  8026   0 44 13   2 0.833 11   2 242
87s107    64 12 44 17   2 1.083 14   3 250
88s006  2191 12 41 14   5 3.000 19   5 942
88s008   150 24 42 12   3 0.667   4   4 228
88s009  1996   0 43 18   4 0.667   8   2 211
1469s4  2827   0 43 24   4 0.917 12   4 250
1469s6  9307   0 44 19   4 1.417 16   1 385;
data lnDummy;
set dummy;
*IF HIC > 300 THEN HIC = 3000;
lhic=log(hic);
lvo=LOG(vo);
lc=LOG(c);
lcdot=LOG(cdot);
lhic2=LOG(hic)-LOG(vi*vi/(64.4*c));
r2=r*r;
vi2=vi*vi;
lCarea=LOG(c_area);
lhic2=LOG((hic*c)/(vi*vi));
proc reg;
model lhic2= r2 s vi2 c_area/P;
*model lhic= r s lCarea/P;
*model lhic= r s lvo lcdot lc/P;
*model lhic2= r2 s vi2 c_area/P;
run;

```

```

*-----*
The following program performs calculations
required to select the best variables for TTI
written by: Monzer Faramawi
date: November 1991
*-----*;
title 'Problem TTI';
data fdays;
input test $ Ln4 r2 vi vi2 vo s c c2 a_r area_c cdot Ln1 Ln2 Ln3;
cards;
91s001 6.498 0 43.8 1918 15 0.9583 1.33 256 4.4 252 22.25 0.19
3.5051 5.6434
91s002 3.696 0 26.17 685 26 0. 0.75 81 2.3 170 12.
-0.48185 2.8854 5.0826
91s003 5.967 0 43.9 1927 12 0.25 0.71 72 2.4 191 11.8 -0.848
2.8663 5.9672
91s004 5. 0 27.75 770 26 0 1.558 351 11.6 350 17.41 0.9942
3.9030 5.8498
91s005 5.881 0 60.8 3696 14 0.583 0.833 100 6.7 258 23.8 -1.22
2.2737 4.8029
91s007 6.973 0 58.35 3404 18 0.167 1.083 169 5.5 271 27
0.4634 3.8682 6.1618
87s096 6.104 0 42 1764 33 0.39 2.167 676 8.3 780 15.7
1.4633 4.9757 7.5514
87s105 7.274 0 44.7 1998 10 0.17 0.792 90 2.3 263 10.15
0.0716 3.8647 7.2742
87s106 6.595 0 44 1936 13 0.2 0.833 100 1.5 242 10.68
-0.0075 3.7105 6.9294
87s107 5.124 1 43.5 1892 17 0.158 1.083 169 3.1 250 13.8 -0.919
2.6696 5.5124
88s006 7.307 1 41.4 1713 14 0.433 3. 1296 4.9 942 19.2 0.9762
4.396 6.6960
88s008 3.914 4 42.3 1789 12 0.275 0.642 59 3.5 228 4.27 -2.8
1.2263 6.1110
88s009 4.975 0 43.4 1883 18 0.33 0.625 56 2 211 8.0
-1.0091 2.8918 6.5965
1469s4 5.587 0 42.8 1831 24 0.316 0.875 110 3.7 250 12.15 0.21989
3.9282 6.9731
1469s6 6.561 0 44.1 1944 19 0.35 1.43 295 1.4 385 16 0.726
4.2607 6.9042;
proc reg;
model Ln1= r2 s c;
run;

```



```

*-----*
The following program performs calculations required to select
the best variables for HIC based on 2500 as upper limit for HIC
    written by: Monzer Faramawi        date: November 1991
*-----*
title 'Problem HIC';
data fdays;
input test $    r2 vi lvi vi2 vo lvo s c c2 rda dam cdot ln1 ln0 ln2
lnvi25 lnvo25 lnvicdot lc lcdot;
cards;
91s001 0    43.8  3.7796 1918 15  2.708 11.5 16    256  4.4  252
22.25  1.5627  5.9865 5.9865 9.46 6.77 4.3566 0.2877 3.13
91s002 0    26.17 3.2646 685  26  3.2581 0    9    81    2.3  170 12.5
3.8728 10.6942 7.824 8.145 8.145 3.6636 -0.2876 2.56
91s003 0    43.9  3.7819 1927 12  2.4849 3    8.5  72    2.4  191 11.8
1.1371 6.2206 6.2206 9.46 6.212 4.0253 -0.2876 2.48
91s004 0    27.75 3.3232 770  26  3.2581 0    18.7 351  11.6 350 17.41
3.9929 7.8292 7.8292 8.33 8.145 3.8066 0.4595 2.83
91s005 0    60.8  4.1076 3696 14  2.6391 7    10    100  6.7  258 23.8
-0.10921 4.9345 4.9345 10.27 6.597 4.4427 -0.1823 3.17
91s007 0    58.35 4.0665 3404 18  2.8904 2    13    169  5.5  271 27
2.999  9.7856 7.824 10.15 7.225 4.4427 0.08 3.29
87s096 0    42    3.7377 1764 33  3.4965 4.7  26  676  8.3  780 15.7
3.1213  8.1271 7.824 9.344 8.741 4.0604 0.77318 2.77
87s105 0    44.7  3.8    1998 10  2.3026 2.12 9.5  90    2.3  263 10.15
2.5133 9.0692 7.824 9.516 5.756 4.0073 -0.1823 2.3
87s106 0    44    3.7842 1936 13  2.5649 2.45 10    100  1.5  242 10.68
2.6535 8.9904 7.824 9.46 6.412 4.0073-0.1823 2.39
87s107 144 43.5  3.7728 1892 17  2.8332 1.9  13    169  3.1  250 13.8
-0.7704 4.1589 4.1589 9.46 7.083 4.06044 0.08 2.63
88s006 144 41.4  3.7233 1713 14  2.6391 5.2  36    1296 4.9  942 19.2
3.2094 7.6921 7.6921 9.283 6.597 4.0943 1.0986 2.94
88s008 576 42.3  3.7448 1789 12  2.4849 3.3  7.7  59    3.5  228 4.27
-1.0784 5.0106 5.0106 9.344 6.212 3.829 -0.4054 1.38
88s009 0    43.4  3.7705 1883 18  2.8904 4    7.5  56    2    211 8.0
2.1559 7.5989 7.5989 9.403 7.225 3.9318 -0.4054 2.07
1469s4 0    42.8  3.7565 1831 24  3.1781 3.8  10.5 110  3.7  250 12.15
2.7866 7.947 7.824 9.403 7.945 4.0073 -0.087 2.48
1469s6 0    44.1  3.7865 1944 19  2.9444 4.2  17.2 295  1.4  385 16
3.0283 9.1385 7.824 9.46 7.361 4.0943 0.3483 2.77;
proc reg;
model ln2=r2 s vi2 carea/P;
%model ln2=lnvi25 lnvo25 s r2 lnvicdot lcdot lc lvo lvi dam cdot/selection=adjrsq;
%model ln2=lnvi25 s r2 lnvicdot lcdot lc lvo lvi dam cdot/selection=adjrsq;
run;

```

References

- [1] M. H. Ray, L. A. Troxel, and J. F. Carney III, "Characteristics of side impact accidents involving fixed roadside objects," *Journal of Transportation Engineering*, vol. 117, May/June 1991.
- [2] "Motor vehicle accident costs," FHWA Technical Advisory T 7570.1, Federal Highway Administration, Washington, DC, June 1988.
- [3] J. D. Michie, "Recommended procedures for the safety performance evaluation of highway appurtenances," Tech. Rep. 230, National Cooperative Highway Research Program, 1981.
- [4] J. R. Hackney, M. W. Monk, W. T. Hollowell, L. K. Sullivan, and D. T. Willke, "Results of the national highway safety administration's thoracic side impact protection research program," *SAE Technical Paper Series*, May 1984.
- [5] NHTSA, "Federal motor vehicle safety standards: Side impact protection," *Federal Register*, vol. 55, pp. 45722-45780, October 30, 1990.
- [6] D. C. Viano, "Biomechanics of injury in lateral impacts," *Accident Analysis and Prevention*, vol. 21, no. 6, 1989.
- [7] I. V. Lau and D. C. Viano, "How and when blunt injury occurs – implications to frontal and side impact," *SAE Technical Paper Series*, October 1988.
- [8] AAAM, "The abbreviated injury scale (AIS-80)," Tech. Rep., American Association for Automotive Medicine, Morton Grove, IL, 1980.
- [9] R. M. Morgan, J. H. Marcus, and R. H. Eppinger, *Side Impact – The Biofidelity of NHTSA's Proposed ATD and Efficacy of TTI*. No. P-189, Society of Automotive Engineers, October 1986.
- [10] T. Gennarelli, H. Champion, W. Sacco, W. Copes, and W. Alves, "Mortality of patients with head injury and extracranial injury treated in trauma centers," *The Journal of Trauma*, vol. 29, no. 9, 1989.
- [11] C. C. Chou, R. J. Howell, and B. Y. Chang, "A review and evaluation of various HIC algorithms," *SAE Technical Paper Series*, March 1988.
- [12] P. Prasad and H. Mertz, "The position of the United States delegation to the ISO working group 6 on the use of HIC in the automotive environment," *SAE Technical Paper Series*, May 1985.
- [13] J. W. Melvin and K. Weber, *Review of Biomechanical Impact Response and Injury in the Automotive Environment*. No. DOT HS 807 042, National Highway Traffic Safety Administration, Washington, DC, 1985.

- [14] J. A. Hinch and D. Stout, *Tests 1785-SI#1-87 through 1785-SI#8-88*. Federal Highway Administration, Washington, DC, 1988.
- [15] J. A. Hinch, J. A. Hansen, M. W. Hargrave, and D. R. Stout, "Full-scale side impact testing," Tech. Rep. FHWA-RD-89-157, Federal Highway Administration, Washington, DC, February 1989.
- [16] T. Turbell, "Eftergivliga belysningsstolpar: Utveckling av en provningsmetod och förslag till krav," Tech. Rep. 204, Staten Väg- och Trafikinstitut (VTI), Linköping, Sweden, 1980.
- [17] J. A. Hinch, G. Manard, D. Stout, and R. Owings, "Laboratory procedures to determine the breakaway behavior of luminaire supports in minisized vehicle collisions," Tech. Rep. FHWA/RD-86/106, Federal Highway Administration, August 1987.
- [18] HNG-21, "Corrugated sheet steel (w-beam) guardrail," Tech. Rep. FHWA Technical Advisory T 5040.23, Federal Highway Administration, Washington, DC, March 13, 1984.
- [19] L. C. Meczkowski, "Evaluation of improvements to breakaway cable terminals," Tech. Rep. FHWA-RD-91-065, Federal Highway Administration, Washington, DC, April 1990.
- [20] M. E. Bronstad and J. D. Michie, "Evaluation of breakaway cable terminals for guardrails," Tech. Rep. 43, NCHRP Research Results Digest, Washington DC, 1972.
- [21] M. E. Bronstad, J. J. B. Mayer, J. James H. Hatton, and L. Meczkowski, "Crash test evaluation of eccentric loader guardrail terminals," *Transportation Research Record*, vol. Roadside Safety, no. 1065, 1986.
- [22] J. G. Pigman, K. R. Agent, and T. Creasey, "Analysis of accidents involving breakaway-cable terminal end treatments," Tech. Rep., Kentucky Transportation Research Program, Lexington, KY, June 1984.
- [23] HNG-14, "Guardrail terminals: Breakaway cable terminal, eccentric loader terminal, and modified eccentric loader terminal," Tech. Rep., FHWA Memorandum to Regional Administrators, Federal Highway Administration, Washington, DC, March 27, 1991.
- [24] S. C. Partyka and W. A. Boehly, *Registration Based Fatality Rates by Car Size from 1978 through 1987*. No. DOT HS 80744, National Information Technical Service, Springfield, VA, 1989.
- [25] NHTSA, "Federal motor vehicle safety standards," Tech. Rep. 208, National Highway Traffic Safety Administration, Washington, DC, March 1971.
- [26] A. H.-S. Ang and W. H. Tang, *Probability Concepts in Engineering Planning and Design*, vol. 1. John Wiley and Sons, Inc., New York, NY, 1975.

- [27] A. A. Afifi and S. P. Azen, *Statistical Analysis*. Academic Press, New York, NY, 1979.
- [28] SAS Institute, Inc., *SAS/STAT User's Guide*, 1991. Version 6.03, Fourth Edition.
- [29] M. H. Ray, J. F. Carney III, M. Faramawi, and L. A. Troxel, "Side impact crash testing," Tech. Rep. draft, Federal Highway Administration, Washington, DC, 1992.
- [30] M. H. Ray and J. F. Carney III, "Side impact test and evaluation procedures for roadside structure crash tests," Tech. Rep. FHWA-RD-92-062, Federal Highway Administration, Washington, DC, 1992.
- [31] H. C. Gabler, J. R. Hackney, and W. T. Hollowell, "Depth: Relationship between side impact thoracic injury and vehicle design," in *Thirteenth International Technical Conference on Experimental Safety Vehicles*, vol. 2, National Highway Traffic Safety Administration, November 1989.
- [32] H. C. Gabler and D. T. Wilke, "Upper interior head impacts: The safety performance of passenger vehicles," in *Thirteenth International Technical Conference on Experimental Safety Vehicles*, no. 91-59-O-07, National Highway Traffic Safety Administration, November 1991.
- [33] N. R. C. Committee on Trauma Research, *Injury In America: A Continuing Public Health Problem*. National Academy Press, Washington, DC, 1985.